Silicon Electrolyte Interface Stabilization (SEISta)

Second Quarter Progress Report 2018

Anthony Burrell
National Renewable Energy Laboratory
15013 Denver West Parkway
Golden, CO 80401
Phone: (303) 384-6666
E-mail: anthony.burrell@nrel.gov

Brian Cunningham, DOE-EERE-VTO Program Manager
Hybrid Electric Systems, Battery R&D
Phone: (202) 586-8055
E-mail: brian.cunningham@ee.doe.gov

Table of Contents

Project Introduction

Silicon is a viable alternative to graphitic carbon as an electrode in lithium-ion cells and can theoretically store >3,500 mAh/g. However, lifetime problems have been observed that severely limit its use in practical systems. The major issues appear to involve the stability of the electrolyte and the uncertainty associated with the formation of a stable solid electrolyte interphase (SEI) at the electrode. Recently, calendar-life studies have indicated that the SEI may not be stable even under conditions where the cell is supposedly static. Clearly, a

more foundational understanding of the nature of the silicon electrolyte interface is required if we are to solve these complex stability issues. A new multi-lab consortium has been formed to address a critical barrier in implementing a new class of materials used in lithium-ion batteries that will allow for smaller, cheaper, and better performing batteries for electric-drive vehicles. This consortium, named the Silicon Electrolyte Interface Stabilization (SEISta) project, was formed to focus on overcoming the barrier to using such anode materials. Five national laboratories, are involved: NREL, ANL, LBNL, ORNL, and SNL.

The SEISta project was developed to specifically tackle the foundational understanding of the formation and evolution of the solid electrolyte interphase on silicon. This project will have as its primary goal an understanding of the reactivity of the silicon and lithiated silicon interface with the electrolyte in lithium-ion systems. It consists of researchers from multiple national laboratories (ANL, SNL, ORNL, LBNL, and NREL) working toward clear unified goals. The Silicon Deep Dive team which is focused upon the science and technology barriers in functional electrodes is a critical partner in this work. Many of the researchers are shared between both teams and we hold joint meetings to ensure effective communication between the teams.

The current goals of SEISta are:

Quarter 1 Milestone:

Have completed the selection and characterization (XPS, SIMS, IR, and Raman), including determination of the surface termination chemistry and impurity levels, of the SEISta model research samples to be used by all members of the team in FY18. (100 % complete)

Quarter 2 Milestone:

Have characterized (XPS, SIMS, IR, and Raman) the surface chemistry and composition of the SEISta model research samples after contact with the electrolyte, before cycling, including the nature of the electrolyte decomposition products. (100% complete)

Quarter 3 Milestone:

Completed characterization (electrochemistry, IR and Raman) of the early stage silicon electrolyte interphase formation on the SEISta model research samples, specifically by establishing and demonstrating a procedure for quantitatively measuring the solubility of SEI on silicon surfaces.

Quarter 4 Milestones:

Established and demonstrated a procedure for measuring the growth rate of silicon SEI components at fixed potentials and during cycling.

Have determined how the physical properties of the silicon electrolyte interface are influenced by the nature of the silicon surface on the SEISta model samples.

Approach

The SEISta team works to ensure that protocols for sample preparation, experimental design and implementation, as well as data reporting are consistent across the whole team. Each laboratory is working toward the same set of quarterly milestones using its own specific talents and capabilities in a concerted effort with the other team members. This joint focus results in multiple researchers interacting to produce and analyze data to ensure that individual experimental variations will not lead to erroneous results. Critical to the success of this effort is the use of standard samples that can be shared by all parties. In the first FY, a round-robin sample test was established to ensure that data could be duplicated at the different laboratories by different researchers. In addition to weekly whole-team video presentations, we have held on-site face-to-face

meetings each quarter for all team members, and other interested parties, to brainstorm and sort out issues with existing experiments and jointly develop new experimental plans.

The outcomes from FY17 indicated that the nature of the silicon starting materials has major implications for the formation and evolution of the SEI. This is most clearly seen in the inherent chemical reactivity of the silicon materials with electrolytes before electrochemistry. Much of our focus for FY18 will be in looking at the initial chemistry of the silicon on contact with electrolytes. This will then lead to an understanding of how the electrode electrolyte interface changes upon applied voltage and how the SEI forms and evolves.

Objectives

The critical issues SEISta is attempting to determine are:

- What are the properties of the lithiated silicon electrolyte interface?
- What is the Silicon SEI actually made of and what reactions are contributing to it?
- How fast does the Silicon SEI grow?
- Does it stop growing?
- Is it soluble?
- Can it be stabilized?

For this quarter the team focused on three broad tasks:

Materials Standardization – This task is critical to the development and deployment of standardized samples and experimental procedures across the team. We will continue to provide full characterization to any new sample that is to be used for SEI studies to ensure reproducibility and full understanding of the material. This Quarters work has focused upon the development of new oxide coatings and methods to control the thickness and density of oxide samples. In addition work on the silicon nano-particles has made progress with the enhancement of the materials collection and handling system in the plasma reactor.

Model Materials Development and Characterization – The nature of the electrode-electrolyte interaction in silicon electrodes is at the heart of the formation and stability of the SEI. The inherent chemical reactivity of silicon with common electrolytes has been a focus for this team and will be a primary focus moving to quarter 2. The synthesis of well-defined silicon nanoparticles and the different chemical markups of lithiated silicon surfaces is being probed by preparing model compounds and thin films that may/can exist in silicon anodes. Lithium silicides, silicates, and other inorganic material (LiF, Li_2O) are being prepared and their reactivity with electrolytes is being determined. These materials also act as standard spectroscopy samples for the researchers who are looking at the formation of the SEI on different silicon materials.

SEI Characterization – The overall objective for SEISta is to understand the nature and evolution of the SEI on silicon anodes. The materials standardization and model compounds will enable the researchers to systematically investigate the formation of the solid electrode interphase using a wide variety of the spectroscopy techniques, from different optical, microscopy, and electrochemistry to determine how the SEI forms based upon the nature of the silicon surface, and how it evolves over time. This section of work will continue to grow in scope as we move beyond the sample characterization phase of the project and on to the understand the nature and evolution of the SEI.

Milestone Quarter 2 FY18: Silicon Electrolyte Interface Stabilization (SEISta)

SEISta Team

Background

The overall objective of the SEISta project is to better understand the formation and evolution of the solid electrolyte interphase (SEI) on silicon anodes. Silicon is a viable alternative to graphitic carbon as an electrode in lithium-ion cells and can theoretically store >3,500 mAh/g. However, lifetime problems have been observed that severely limit its use in practical systems. The major issues appear to involve the stability of the electrolyte and the uncertainty associated with the formation of a stable solid electrolyte interphase (SEI) at the electrode. Recently, calendar-life studies have indicated that the SEI may not be stable even under conditions where the cell is supposedly static. Clearly, a more foundational understanding of the nature of the silicon electrolyte interface is required if we are to solve these complex stability issues. A new multi-lab consortium has been formed to address a critical barrier in implementing a new class of materials used in lithium-ion batteries that will allow for smaller, cheaper, and better performing batteries for electric-drive vehicles. This consortium, nicknamed the Silicon Electrolyte Interface Stabilization (SEISta) project, was formed to focus on overcoming the barrier to using such anode materials. Five national laboratories, led by the National Renewable Energy Laboratory (NREL), are involved: NREL, as well as Argonne (ANL), Lawrence Berkeley (LBNL), Oak Ridge (ORNL), and Sandia National Laboratories (SNL). The second quarter milestone for SEISta in FY18 was:
To have completed the selection and characterization (XPS, SIMS, IR, and Raman), including determination of the surface termination chemistry and impurity levels, of the SEISta model research samples to be used by all members of the team in FY18.

Results

This objective was 100% completed.
Several different research samples are used as standard materials in the SEISta project. In FY17 we discovered that the inherent chemical reactivity of silicon and silicon oxides with common organic molecules has a profound effect on the surface of the silicon even before electrochemistry begins. In addition, many of phases that are suspected to form during electrochemical cycling have their own reactivity. The quarter 2 millstone directly relates to the need for a more comprehensive understanding of the surface chemistry of the silicon that provides the foundation for the SEI.

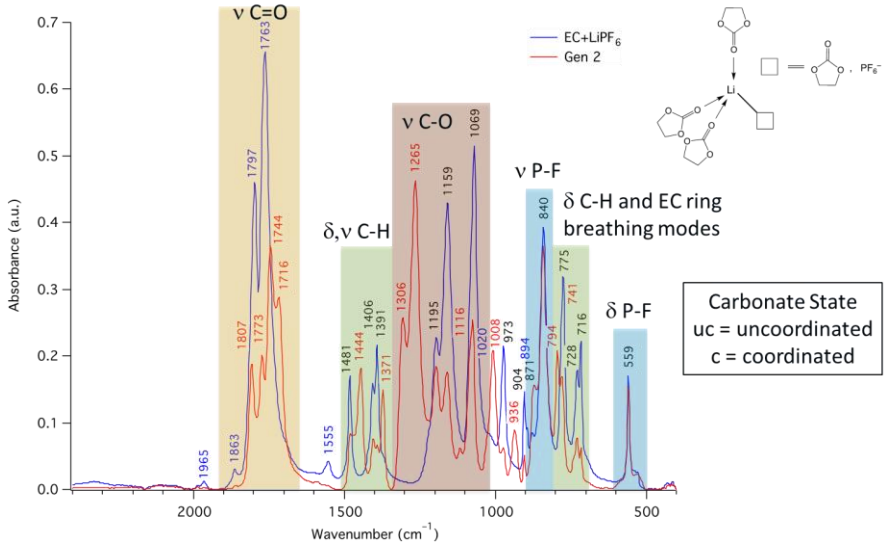

Figure 1 FTIR data and assignment for the .2M LiPF6 in EC:EMC 30:70 wt% electrolyte

The approach begins with a spectroscopic characterization of the products formed by contacting our baseline samples with the standard electrolyte formulation (1.2M LiPF6 in EC:EMC 30:70 wt%). In addition, some

characterization of the reactivity of standardized samples with the Silicon Deep Dive were carried out (1.2M LiPF6 in EC:EMC 30:70 wt% with 15wt% FEC). The initial characterization of the reaction products used a combination of XPS, FTIR, GC-MS and molecular dynamics to determine the specific nature of the reactive and reacted species. Figure 1 contains the preliminary assignment of the vibrational spectrum of the SEISta baseline electrolyte. After exposure to the electrolyte there are marked changes present in the spectrum as seen in figure 2.

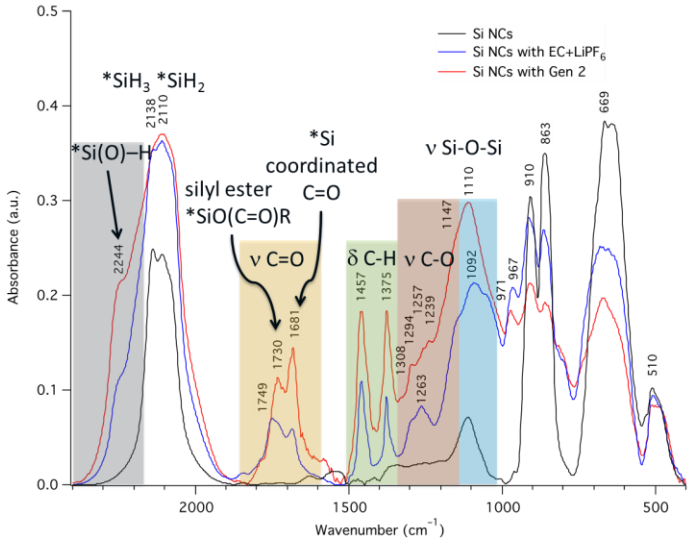

Figure 2 the FTIR spectra of the bare silicon nano particles before and after contact with the SEISta electrolyte and a mixture of EC and 1 molL^{-1} PF_6.

In addition to the reactivity volatile components that were produced during the reaction in a pseudo in situ-IR cell. This not only enables detection of specific components it also allows for the collection of kinetic data and when coupled with a GC-MS specific mass determinations as seen in figure 3.

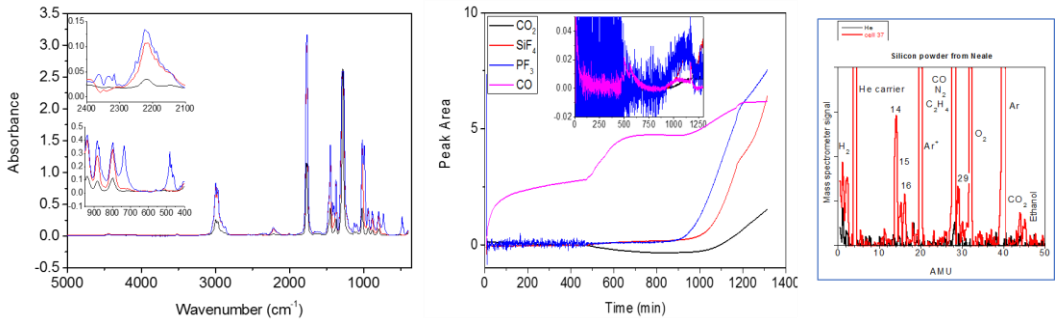

Figure 3 Gas data collected on the reactivity of silicon samples.

Following the experimental FTIR characterization, we have utilized molecular dynamics to conduct parallel simulations, which confirmed the existence of both contact ion pair and solvent separated ion pair solvation structure in the bulk electrolyte. The calculated spectrum results accord well with the experimental results. Furthermore, reduction potential calculations, including the full speciation of the electrolyte, are being conducted, which offers a theoretical explanation of the influence of the FEC additive. Further reduction reaction calculation will be conducted to explain the reduction mechanism and the formation path for LiF, LiEDC, LiSixOy, Lithium ethylene dicarbonate and other SEI components. Additionally, vibrational spectra of predicted SEI components have been computed using density functional perturbation theory to confirm experimentally assigned vibrational modes and frequencies. Model carboxylates (such as EC and DMC) adsorbed to a Si-Ox surface (figure 4) exhibit vibrational modes in agreement with experimental FTIR assignments.

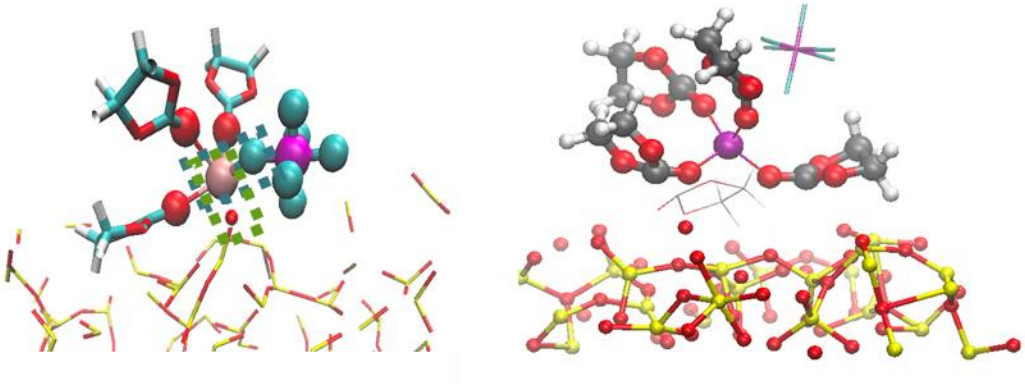

Figure 4 Interface simulation for electrolyte in the region within 4 Å from the SiO2 surface

A series of samples of a thermally grown 50-nm SiO_2 layer on top of a Si wafer were investigated to understand the reaction with simple electrolytes. The electrolytes selected were the standard, 'GEN2' electrolyte (1.2M LiPF6 EC:DMC) and an electrolyte with an FEC additive (1.2M LiPF6 EC:DMC with 10wt% FEC). Each sample was freshly made, then exposed to a drop of electrolyte that completely covered the surface for 30 m. The sample surfaces were washed with DMC to rinse off any salt residue that might have dried on the surface. After rinsing, the samples were immediately transferred without air exposure to a glovebox connected XPS system for analysis. The data in figure 5 demonstrates evidence that Li-containing Si-based electrodes drive electrolyte decomposition reactions at the electrode surface. By comparison, SiO_2 layers on Li-free Si electrodes appear to be etched, by the electrolyte solution, leaving behind Si and a surface layer consisting of adsorbed organics. Furthermore, this behavior in the Si-only electrodes is observed for both the GEN2 electrolyte and the electrolyte containing an FEC additive.

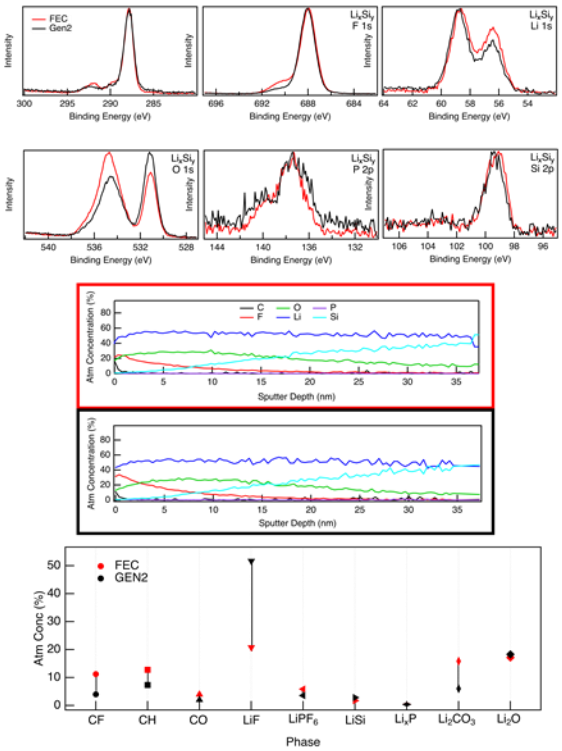

Figure 5. XPS data showing effects of electrolyte exposure on lithium silicide electrodes

Reactivity studies of a number of silicon samples were carried out and the complete data is in the process of being submitted for publication. Much of the data associated with these studies are presented below.

Conclusions

The milestone was 100% completed with an extensive characterization of the reactivity of the standardized samples within SEISta being examined. There is significant evidence that the nature of the silicon-electrolyte interface is directly dependent upon these initial reactions. Over the rest of this year we will probe the influence of this reactivity with respect to the formation and stability of the silicon -electrolyte interface.

Materials Standardization: Electrochemical Testing of Silicon Wafer Anodes – Doping and Corrosion (NREL)

Manuel Schnabel (NREL), Matt Page (NREL), Paul Stradins (NREL)

Background

Polished silicon wafers provide the most controlled silicon material with which to study the fundamental processes occurring during the lithiation of silicon from an electrolyte. We have previously reported on a cleaning routine adapted from the electronics industry that was applied to hundreds of samples for round robin measurements within this project, as well as on a method to prepare oxidized silicon surfaces with precisely controlled SiO_2 thicknesses, and on improving the rear side contact to the silicon.
This quarter, we have used these techniques to prepare phosphorus (n-type) and boron (p-type) doped wafer pieces, and prepared coin cells to compare their performance. Furthermore, we have improved the low-current capability of our cycling station to facilitate low-current corrosion experiments in FY18Q3.

Results

1. **N-type and p-type Si wafers** are, a priori, expected to behave differently in an electrochemical cell because their bulk work functions differ by about 1eV. To test this, as well as the indium soldering approach we developed last quarter for effectively contacting Si, we assembled coin cells with n-type and p-type wafers (n, p), with and without In solder contacts (nI, n; pI, p). The cells were half-cells against Li metal. To our surprise, we found that all cells had open-circuit potentials between 2.4 and 2.7V, regardless of doping. Cyclic voltammetry results for the first 10 cycles are shown in Fig. 1.

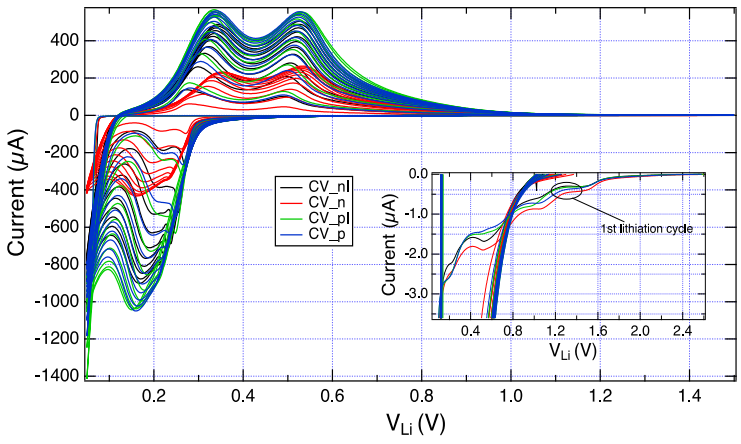

Figure 1: Cyclic voltammetry (0.5mV/s, 1.5V-0.05V) of half cells with both n-type and p-type anodes, both with (suffix "I") and without a soldered indium contact. The inset shows the small peaks during the first half cycle.

We see that all cells exhibit the same main peaks, and that peak positions for n-type samples are not systematically different to those of p-type samples (one exception being a <1µA peak at ~0.55V vs Li observed during the first lithiation cycle, see inset, which may be related to an electrolyte reduction reaction that occurs only at n-type Si). This suggests that perhaps the surface work function, which is relevant to electrochemistry, is similar for n-type and p-type wafers. However, the main peaks for sample "n" are much smaller than for the other samples and shift more strongly to more extreme voltages (lower voltages for lithiation, higher voltages for delithiation) with increasing current. We also cycled the cells galvano-statically and saw that cell "n" required more extreme voltages at any given point within a lithiation cycle.
This suggests a higher resistance in this cell and shows that even at doping levels of $1.3x10^{19}$ cm^{-3}, at which Si is nominally metallic, making a good contact to Si, e.g. by using indium, is critical in order to measure the interference-free behavior of the anode ("nI", as compared to "n"). Conversely, a doping level of $1x10^{20}$ cm^{-3}, which the p-type samples had, seems to be sufficient to make a soldered indium contact unnecessary for accurate electrochemical measurements.

2. **Measuring background currents** (electrolyte reduction or anode corrosion) at voltages where no lithiation/delithiation takes place can require the measurement of very small currents. To improve the low-current capability of our cycling station, we built a Faraday cage to house the cell, and tested it using chronoamperometry with a 10 MΩ resistor.

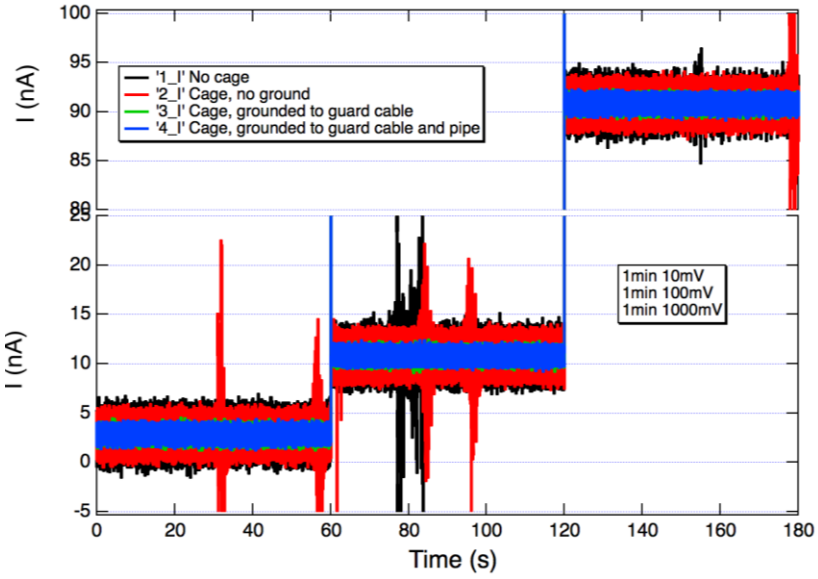

Figure 2: Current through a 10 MΩ resistor as a function of time, for 1min at 10mV, 1min at 100mV, 1 min at 1V.

As can be seen in Figure 2, the measurement is initially quite noisy (black). Simply using the Faraday cage has little effect (red), but when the cage is grounded, it reduces noise in the measurement by more than half. Interestingly, grounding it to the guard cable of the potentiostat is sufficient, demonstrating that the potentiostat itself is well grounded. The remaining noise is below the specifications of the manufacturer, and a low current circuit board has been ordered that ought to allow measurements down to 1pA. Implementing and utilizing this new hardware will be a key objective for the next quarter.

Conclusions

The electrochemical performance of n-type and p-type silicon was compared. The nominally different work function had no clear effect, but the lower doping of the n-type wafers demonstrated that soldered contacts are required for acceptable contact resistance up to doping levels approaching 10^{20} cm^{-3}. A Faraday cage to suppress noise in low current measurements has been constructed, and will be combined with low-current circuitry in the coming quarter.

Materials Standardization: Chemical and Electrochemical Reactivity of Plasma-Synthesized Silicon Nanoparticles

Bertrand Tremolet de Villers, Gregory Pach, Nathan Neale (NREL)

Background

One of NREL's tasks explores plasma-synthesized silicon nanoparticles (Si NPs) as model systems for Li_xSi anodes. Such plasma-prepared Si NPs are valuable since they feature hydrogen-passivated surfaces and a high surface area resulting from their <10 nm diameter that makes them well suited for chemical reactivity studies using Fourier transform infrared (FTIR) spectroscopy and quantitative off-gassing analysis. These reactivity studies are relevant for understanding (1) early-stage SEI layer growth as well as (2) individual SEI component chemical stability. In FY17, we prepared several ~100 mg batches of ~7 nm diameter Si NPs for chemical reactivity studies. Making larger diameter (10–200 nm) Si NPs and at a greater scale (>100 mg) as well as extending chemical reactivity to electrochemical reactivity are key objectives in FY18.

Results

In Q2 FY18 we operated at full staffing that resulted in significant progress toward year-end goals:

1. Expand existing RF plasma reactor to produce larger Si nanoparticles (NPs) and at greater scale
    a. Subtask FY18 Q4 Milestone: 30–50 nm diameter and 0.5–1.0 g (per basket)
2. Use Si NPs as high surface area model systems for:
    a. Chemical reactivity studies
    b. Electrochemical reactivity studies

Tasks 1 & 2 ultimately will enable the evaluation of plasma-synthesized Si NPs in batteries both with and without surface modifications. Modifications could include both molecular functionalization (e.g., alkoxides, fluorinated hydrocarbons/alkoxides) or inorganic coatings (e.g., oxides, nitrides, carbides). In FY18 we are establishing the baseline chemical and electrochemical reactivity of plasma-grown Si NPs. Essential to these tasks is the ability to scale up our process to battery-relevant quantities as well as sizes an order of magnitude greater than we had produced prior to the SIESta project.

Significant effort in Q2 was spent exploring the plasma growth conditions, and those activities will continue for the duration of FY18. Initial results are promising in that we have already found that residence time of the gas in the active plasma regions is only one of several factors that control the Si NP size. As silane gas enters the plasma, it is fragmented into atomic subunits that then for nanoparticle nuclei (molecular clusters and very small nanoparticles). These nuclei coagulate into large particles through collisions. Subsequently, nanoparticles surface growth occurs by reaction with remaining precursor or with precursor that is replenished in the reactor.[1] The residence time is known to have a strong influence on the NP size particularly through this 3rd stage of NP surface growth, with longer residence times providing larger particles. The residence time is directly proportional to the plasma volume ($\pi r^2 h$) and pressure (P) and inversely proportional to the total gas flow rate:

$$Residence\ Time = \frac{\pi r^2 h P}{flow\ rate}$$

This brings up an interesting conundrum: Higher yield per unit time is achieved by increasing all gas flow rates. However, as seen from the equation, this will decrease the residence time and thus decrease Si NP size. Therefore, the plasma volume and pressure need to be increased to account for the increased gas flow rate. Our new reactor setup with a 19 mm ID reactor tube provides a large volume and the ability to explore a wide range of pressures (1–100 Torr) and gas flow rates (20–1000 sccm). We have found that other reactor parameters significantly affect Si NP size. For example, the plasma power density, which we previously identified can be used to tune the Si NPs from amorphous (a-Si) to hydrogenated (a-Si:H) to crystalline (c-Si), also impacts the crystallite size as shown in Table 1. Note also that our typical size determination based on XRD spectra Scherrer analysis of peak width is approaching its limits (i.e., particles become indistinguishable from bulk due to linebroadening effects). We will need to partner with the rest of the SEISta team to being to characterize Si NP size through TEM imaging going forward. This also will be important as we are currently only measuring primary crystallite size, not actual particle size, using XRD.

Table 1. Impact of Plasma Power Density on Si NP primary crystallite size. Samples A–D were grown under identical conditions (pressures, flow rates, etc.) besides the power density.

Sample	Forward Power (W_f)	Delivered Power Density (W cm^{-3})	Crystallite Size from XRD (nm)
A	250	2.4	18
B	200	2.1	16
C	150	1.6	16
D	100	1.1	13

This type of sweep of a wide range of parameters is enabled by the successful scale-up of our multi-sample load lock collection system. As shown in Figure 1, up to 5 unique samples can be collected in a single production run. This high throughput allows us to quickly explore the effect of various reactor parameters. In subsequent quarters, we will be exploring the effect of pressure as well as the ratio of gas mixtures. Currently we have two different silane sources: 10% SiH_4 in He, and 100% SiH_4. Typically, we flow 3–6% SiH_4 in a mixture of He and Ar carrier gases. The Si NPs pictured in Figure 1 with sizes detailed in Table 1 were grown instead with 17% SiH_4 in exclusively Ar carrier gas. Hydrogen also can be added to change the surface chemistry and modulate the size to a degree. We also have the ability to introduce a second gas flow downstream of the working and ground electrodes termed the "afterglow" region. We will be exploring the effect on size of introducing additional SiH_4 gas flow into the afterglow to replenish precursor during the NP surface growth phase.

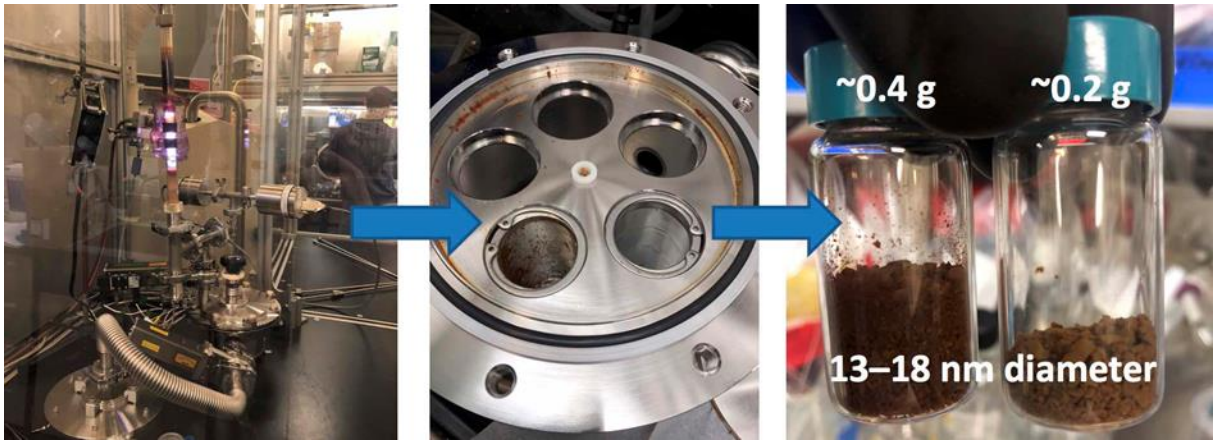

Figure 1. Left: Scaled-up plasma reactor during Si NP production run; Middle: Multi-sample collection system; and Right progress toward tuning plasma growth conditions toward increased Si NP size and yield.

Next, we have continued to work with partners on manuscripts detailing Task 2a: Chemical reactivity studies of SEISta model samples including Si NPs, SiO_x NPs, and Li_2SiO_3 and Li_4SiO_4 particles. A complementary gassing study with SEISta partner Gabriel Veith (ORNL) was performed in which the gaseous product from these reactions were quantified using gas chromatrography-mass spectrometry (GC-MS). This ORNL study on NREL's Si NPs as well as in-house prepared lithium silicates and silicon oxides corroborates our FTIR chemical reactivity study. We expect to submit both of these publication for peer review in Q3 FY18.

Finally, we made significant progress in Q2 FY18 toward building a new in operando ATR-FTIR electrochemical instrument to accomplish Task 2b: Electrochemical reactivity of SEISta model samples. As noted in our Q1 FY18 report, we worked extensively with Dr. Phil Ross (LBNL) given his extensive prior work in this area[2,3] to ensure the validity of the design and have ordered the necessary hardware for our existing FTIR spectrometer. Pike Technologies was identified as having the best combination of ATR capabilities that will interface with an existing Nicolet 6700 FTIR spectrometer. The necessary Nicolet inert, alignment fixture, electrochemical cell, and ZnSe ATR crystals were purchased. We developed a custom air-free cell that allows us to access a Si wafer surface electrochemically, and performed initial experiments using this ATR-FTIR-electrochemical setup. We have been able to use the EChem cell to successfully cycle a planar Si wafter anode in this 2-electrode setup (Li foil CE/RE) and observe the SEI ex-situ. We are currently working on optimizing the Si wafer to balance the competing trade-off between resistivity and IR transmittance. Lightly-doped Si wafers with carrier densities ~10^{15} cm^{-3} provide good IR transmission, however are somewhat resistive (1–5 Ω cm). In contract, highly-doped Si wafers with carrier densities ~10^{18} cm^{-3} provide poorer IR transmission but are much less resistive (1–5 mΩ cm). The wafer thickness also is an important factor, with 1 mm thick wafers offering poorer transition but better structure stability than thinner (100–300 μm thick) wafers. Another option we will be exploring in the rest of FY18 is to work with SEISta collaborators to deposit model samples (e.g., 50 nm thick Li_xSi) *directly* onto the ZnSe ATR crystal.

Figure 2. Left: Li foil CE/RE on stainless rod contact within the electrochemical (EChem) cell; Middle: Assembled EChem cell on the ZnSe ATR crystal (on bottom plate under the EChem cell, not shown); and Right: EChem cell on the variable angle ATR module within the FTIR spectrometer.

Conclusions

Key findings in this reporting period are:

- Scale-up of Si NPs is in progress, with reasonable yields (0.2–0.4 g per basket; 1–2 g per production run) and increased sizes than we have grown previously (13–18 nm diameter primary crystallite size).
- Progress on our in operando ATR-FTIR-electrochemical setup is progressing as expected, with some learning curve but good initial results.

Future FY18 efforts will be devoted toward continuing to explore the parameter space to increase Si NP sizes and yields further, as well as to further refinement of our in operando ATR-FTIR-electrochemical instrument.

References

1. Kortshagen, U.; Sankaran, R. M.; Pereira, R. N.; Girshick, S. L.; Wu, J. J.; Aydil, E. S. *Chem. Rev.* **2016**, *18*, 11061.
2. Shi, F.; Ross, P. N.; Zhao, H.; Liu, G.; Somorjai, G. A.; Komvopoulos, K. *J. Am. Chem. Soc.* **2015**, *137*, 3181.
3. Shi, F.; Ross, P. N.; Somorjai, G. A.; Komvopoulos, K. *J. Phys. Chem. C* **2017**, *121*, 14476.

Materials Standardization: Fabrication of ^{18}O labeled Si/SiO_2 electrodes

Gabriel M. Veith (ORNL), Steven Harvey, Kevin Wood (NREL)

Background

One of the unanswered questions regarding the interfacial chemistry of silicon is what is the role of the SiO_x surface termination layer on the SEI formation reaction, lifetime, and cycleability? Thus far there have been multiple sets of conflicting information regarding the influence of the SiO_2 and if this SiO_2 reacts to form a lithium silicate on the Si surface. There is infrared and NMR spectroscopy data which shows with cycling the growth of Li-Si-O species. In contrast, X-ray absorption data shows the absence of Li-Si-O with cycling.

The goal of this work is to identify the presence/absence of Li-Si-O and identify its location on the electrode and role in SEI formation. To accomplish this, we are performing experiments using ^{18}O terminated silicon electrodes. The benefit of this isotope labeling is that it will enable us to identify where the potential Li-Si-O is forming AND where the oxygen used to form the Li-Si-O materials comes from. Specifically, oxygen from the termination of the silicon electrode or oxygen from the carbonate solvent used in the electrolyte. In addition to the ^{18}O labeling samples of pure Li-Si-O are being prepared for comparison and thin film electrodes are being fabricated to support the corrosion current fundamental question.

Results

To accomplish this goal a vacuum chamber at ORNL was modified to allow selective addition of ^{18}O enriched gas, Figure 1(left). These modifications required gas handling systems to deliver the oxygen gas to the sputter target to form the $Si^{18}O_2$ depositing layer. Several test runs were performed to evaluate the test parameters.

Figure 1(right) shows Time-of-flight-secondary-ion-mass spectrometry (TOF-SIMS) data collected for the final test sample of a film deposited on the standard battery grade copper foil. This data shows an ion profile as a function of depth. From the data it is clear the surface is terminated with ^{18}O (pink line). The concentration of the Si changes with depth (red line) due to the evolution from SiO_2 to Si as the sputtering process penetrates the film confirming the film structure. One also notices (teal line) the presence of the $^{16}O^-$ species which appears to have two features: a signal at the surface from impurities in the ^{18}O sputter gas or reaction with oxygen/water in the air and a second hump at the copper surface due to the presence of copper oxide. This feature will be important for future characterization to identify if the Si/Cu interface is changing with cycling.

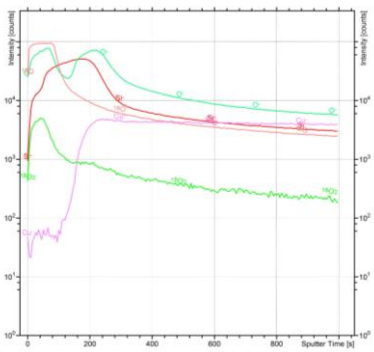

Figure 1. Picture of the modified deposition system used to prepare the ^{18}O labeled Si/SiO_2 films (Left); TOF-SIMS data collected for the test samples demonstrating the surface is terminated with ^{18}O before the growth of the Si working electrode on the copper foil substrate.

Conclusions

Materials are being prepared and shipped to partner labs for analysis.

Model Materials Development and Characterization: Understanding Surface Reactions of Si Electrodes Upon Contact with Electrolyte

National Renewable Energy Laboratory: Interfacial and Surface Science Group
Glenn Teeter
Steve Harvey
Kevin Wood

Background

The reactivity of Si-based anodes causes problems for reproducibility and reliability of Si-based battery systems. Unfortunately, detailed experiments showing how the surface of well-controlled model electrodes react with the electrolyte before cycling is lacking in the literature. Furthermore, it is typically assumed that the oxide on the Si surface plays an important role determining SEI species and performance.

- *Key goal: understand the reactivity of model Si Anode materials when in contact with electrolyte*

Results

To investigate the effects of electrolyte contact on the surface of Si anode materials, three model electrode systems were selected and reacted with two different electrolytes. The model electrodes chosen where evaporated Li_7Si_3, a sputter-deposited Si thin Film, and a thermally grown 50-nm SiO_2 layer on top of a Si wafer. The electrolytes selected were the standard, 'GEN2' electrolyte (1.2M LiPF6 EC:DMC) and an electrolyte with an FEC additive (1.2M LiPF6 EC:DMC with 10wt% FEC). Each sample was freshly made, then exposed to a drop of electrolyte that completely covered the surface for 30 m. The sample surfaces were washed with DMC to rinse off any salt residue that might have dried on the surface. After rinsing, the samples were immediately transferred without air exposure to a glovebox connected XPS system for analysis.

For the Li_7Si_3 samples obvious differences can be observed between the FEC soaked and GEN2 soaked samples (Figure 1). These differences can be summarized as: the FEC soaked samples exhibits less LiF (GEN2: 51.7%, FEC: 20.8%), while the GEN2 sample exhibits fewer organic species on the surface (i.e., C-F, C-H, C-O, etc.). These results are intriguing because the FEC electrolyte is known to outperform the GEN2 electrolyte, but conventional wisdom typically infers that more inorganic compounds lead to a better behaving SEI. Despite this fact, the improved behavior of the FEC electrolyte could be attributed to the possibility that the FEC reacts more uniformly with the electrode, leads to a more uniform flux of Li ions across the interface (causing a lower effective current density). Further studies, included spatially resolved measurements are planned to better interpret these results.

For the Si-only electrodes (initially Li-free), the surface layer was significantly different. The approximate thickness of the decomposed electrolyte on the Li_7Si_3 was around 30 nm, while on both the Si thin film and Si wafer samples the SEI consisted of only a monolayer of adsorbed organics (C,O and F) and no appreciable amount of Li (Figure 2). Furthermore, the oxide layers on both Si-only electrodes disappeared. For the Si thin film sample no SiO_x phase was even observed, while in the case of the 50 nm thermally grown SiO_2 layer on Si, only a small amount of SiO_2 was observed at the surface. Then upon sputtering, that SiO_2 phase completely disappeared after less than 30 s of sputtering (< 2 nm). Moreover, there are no obvious or significant

differences between the FEC and GEN2 electrolytes. These results are surprising and likely indicate that water contamination in the electrolyte leads to HF formation, which in turn etches the surface oxide.

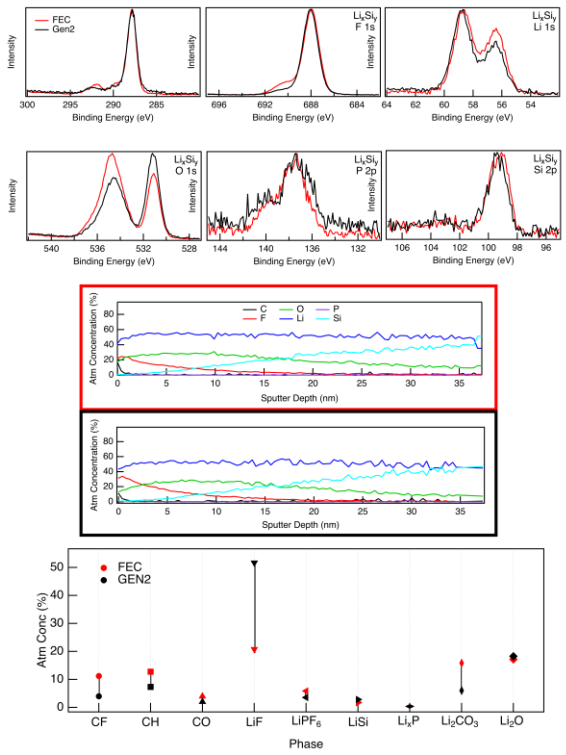

Figure 1. XPS data showing effects of electrolyte exposure on lithium silicide electrodes.

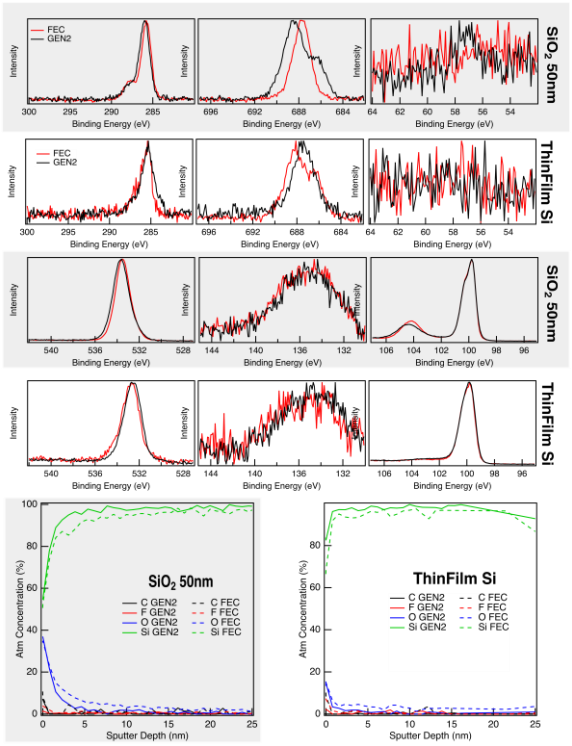

Figure 2. XPS data showing effects of electrolyte exposure on Si-only electrodes.

- *Lithium silicides react upon contact with the electrolyte to form an SEI-like layer.*
- *When lithium silicide comes in contact with an FEC containing electrolyte, less LiF is formed and a higher percentage of organics appear on the surface than for a GEN2 electrolyte.*
- *Si-only electrodes exhibit a very small amount of electrolyte decomposition onto the surface of the electrode; only a monolayer of adsorbed organics is observed.*
- *Oxides on the surface of Si-only electrodes are removed upon contact with both electrolytes tested, this presumably occurs due to water contamination within the electrolyte that creates HF.*

Conclusions

In summary, we have observed evidence that Li-containing Si-based electrodes drive electrolyte decomposition reactions at the electrode surface. By comparison, SiO_2 layers on Li-free Si electrodes appear to be etched, by the electrolyte solution, leaving behind Si and a surface layer consisting of adsorbed organics. Furthermore, this behavior in the Si-only electrodes is observed for both the GEN2 electrolyte and the electrolyte containing an FEC additive. Conversely, the FEC additive appears to make a difference in the decomposition product on the surface of Li-containing Si electrodes, by reducing the amount of LiF and increasing the amount of organic functionalities.

The electrode surface drastically changes after contact with the electrolyte: in Li-containing Si electrodes an electrolyte decomposition reaction occurs, while in the Si-only electrodes a reaction occurs that etches the electrode surface.

Model Materials Development and Characterization: Inherent Reactivity Studies of Lithium Silicides

Baris Key (ANL), Binghong Han (ANL), Fulya Dogan (ANL), Chen Liao (ANL), Jack Vaughey (ANL)

Background

One of the core problems associated with Li-Si chemistry in a Li-ion battery is the inherent reactivity of the lithium silicides, the active material that forms upon the lithiation. These phases can react with almost all battery components such as binders, electrolytes, additives and impurities such as moisture and air which cause major columbic losses and loss of lithium.

Results

A synthetic and characterization effort was undertaken to prepare key model compounds in the Li-Si phase diagram. Based on previous work, lithium and silicon order can be assigned to main and impurity phases effectively (1-3). So far, X-ray diffraction and Solid State Magic Angle Spinning (MAS) NMR spectroscopy have been used to qualitatively and quantitatively to probe reactivity of the model compounds with typical binders used in Li-ion cells. NMR spectroscopy has previously been shown (1,2) to effectively study the Li and Si ordering in amorphous and crystalline phases of lithium silicides. With the help of these earlier efforts, the trends in ^{7}Li and ^{29}Si NMR is used to follow the Li and Si inventory quantitatively pre and post treatment with cell components such as electrolytes and binders (previously reported in a quarterly report). An imperfect attempt using static NMR technique to quantify the reactivity of Li_7Si_3 vs. carbonates, sulfones and glymes showed that exposure to triglyme induced least structural change and Li-loss (reported in Q1 FY'18).

The technique is improved with the application of an in-situ MAS NMR technique, generating unprecedented resolution comparing the bulk reaction between EC, EMC, FEC and Triglyme solvents and freshly prepared Li_7Si_3 as shown in Figure 1a. The results show highest Li loss and bulk reaction for EC and lowest for Triglyme confirming the static NMR results conclusively. Interestingly FEC and EMC also showed only slight reactions and positive Li shift indicating relative inertness. Furthermore no LiF formation was detected in the FEC experiment, contrary to common belief that FEC defluorination reaction would be prevalent in the presence of lithium silicides. The FEC results suggest either Li_7Si_3 of about 300-400mV potential vs. Li is not reducing enough and/or a flow of electrons is also required for FEC passivation reaction. **The reaction vs. $Li_{13}Si_4$ will be monitored in the next quarter to investigate the former. The EMC results suggest new carbonate electrolyte formulations excluding EC could improve coulombic efficiency of the system and will be the focus of new electrochemical tests in the next quarter**.

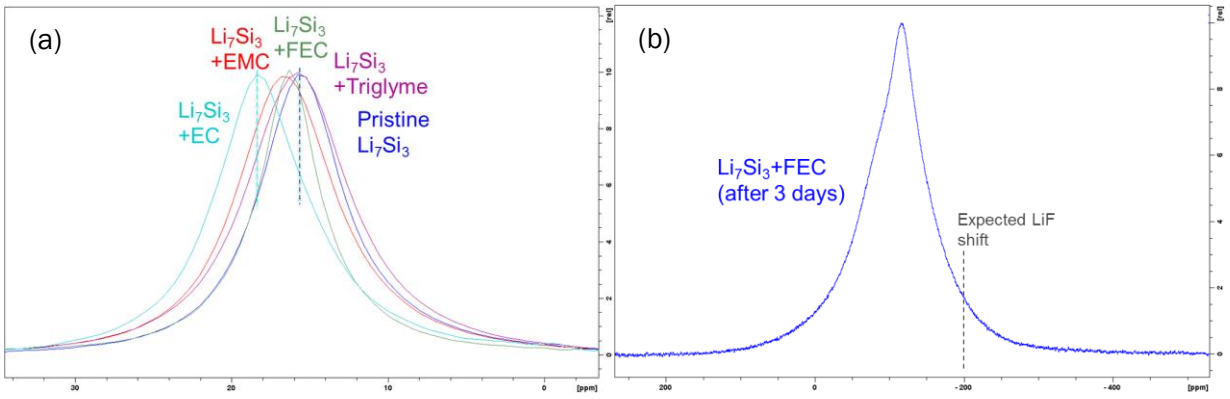

Figure 1. (a) ^{7}Li in-situ solid state MAS NMR for Li_7Si_3 and electrolyte solvents (b) ^{19}F in-situ solid state MAS NMR for Li_7Si_3 and FEC. ANL, unpublished results

Based on the reactivity study results and lack of literature results on glymes and silicon electrodes a preliminary test of the electrochemical performance of a triglyme electrolyte formulation (1M LiTFSI in triglyme) was also studied via a simple baseline silicon powder and hard carbon mixture in half cells. The 1st cycle electrochemical performance, shown in Figure 2a, was about 75% higher in both discharge and charge capacities vs. the baseline electrolyte. This result alone is consistent with the hypothesis that the inertness of the electrolyte system could minimize side reactions and improve the overall capacity that can be obtained

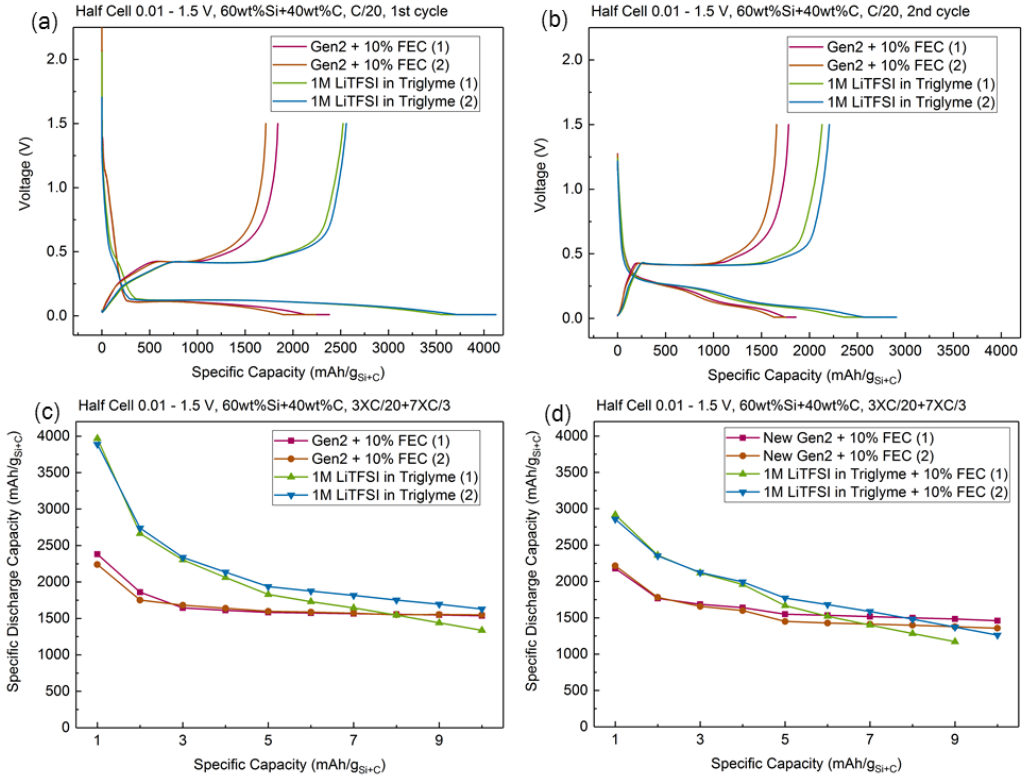

Figure 2. Electrochemical profiles of Paraclete baseline silicon powder and carbon SP electrodes vs. Li metal half cells comparing Gen2 + 10% FEC and 1M LiTFSI in Trigylme electrolytes. ANL, unpublished results

from silicon. Figure 2a and 2b also show the overall electrochemical profile comparison of the new electrolyte vs. the baseline and suggest no major changes in the overall lithiation and delithiation electrochemistry. Figure 2c shows the comparison of cycle life behavior for the two electrolyte systems. While the baseline electrolyte capacities are lower in the first few cycles, they rapidly stabilize and are consistent for 10+ cycles whereas the triglyme electrolyte performances are never found to stabilize and decay fast. This behavior could be explained by a lack of passivation on the electrode surface and/or Li-salt side reactions on the Li metal. Figure 2d illustrates an attempt to simply incorporate a passivation aid, FEC, to the system, which did not improve the performance. **The results prompt basic characterization studies to study the reactions above with full cell electrochemistry, NMR, microscopy, FTIR and XPS which will be the focus in the next quarter.**

Conclusions

Quantification of the reactivity of Li_7Si_3 vs. carbonates (EC, EMC and FEC) and triglyme showed that exposure to triglyme induced least structural changes and Li-losses whereas FEC and EMC reactions are relatively subdued and reaction with EC is most pronounced. No LiF formation is detected for FEC. A glyme

based electrolyte was prepared which initially outperforms the baseline by 75%. However, electrochemistry results suggest that interface passivation for this formulation is inadequate and cell performances decay rapidly. Therefore basic characterization experiments and tests with Li-rich model compounds are in progress to explore the potential of new electrolyte formulations based on the results.

References

1. B. Key, R. Bhattacharyya, M. Morcrette, V. Seznec, J-M. Tarascon, C. P. Grey, J. Am. Chem. Soc., 2009, 131 (26), pp 9239–9249
2. B. Key, M. Morcrette, J-M. Tarascon, C. P. Grey, J. Am. Chem. Soc., 2011, 133 (3), pp 503–512
3. Multinuclear Solid-State Nuclear Magnetic Resonance of Inorganic Materials, Volume 6, 1st Edition, Authors: Kenneth MacKenzie M.E. Smith

Model Materials Development and Characterization: SEISta – Fluorescent probes (NREL) (FY18 Q2)

Contributors (NREL – Wade Braunecker)

Background

Last quarter, some initial experiments were described where a Li ion fluorescent probe was covalently tethered into two different model binder systems commonly employed with silicon anode materials. Some initial characterization was performed, which demonstrated the sensitivity of this probe's absorbance/fluorescence spectra to Li ion concentration. We ultimately aim to develop fluorescent probes that will help determine how components of the silicon SEI layer evolve with cycling. The work will specifically contribute to SEISta project milestones by complimenting existing strategies to quantitatively measure soluble components of the SEI as well as measure the growth rate of the SEI components at fixed potentials and during cycling.

During the recent face-to-face meeting in January, Jagit Nanda (**ORNL**) and Robert Kostecki (**LBNL**) helped identify that (depending on the cathode and electrolyte employed) the silicon anode SEI layer can be fluorescent in and of itself. Thus, we determined it will be important that we have the ability to "tune" the wavelength at which the Li ion probes fluoresce. To that end, on our synthetic progress in February and March following the face-to-face meeting is reported here.

Results

We designed and implemented experimental routes for the synthesis of two new Li ion fluorescent sensors based on a modified literature design for tuning chromophore fluorescence.[1] The strength of the different electron donating and withdrawing groups on monomers M1 and M2 (Scheme 1) will in principle allow the emission spectra of these compounds to be tuned so they do not significantly overlap with the background fluorescence of the SEI layer. As these compounds have not previously been reported in the literature, synthetic procedures were refined for each step. The synthesis of M1 and M2 is nearly complete, after which we will probe how the internal "push-pull" effect of the electron donating/withdrawing groups affect mechanisms of fluorescence and the sensitivity of the molecules to Li ions in various relevant reaction

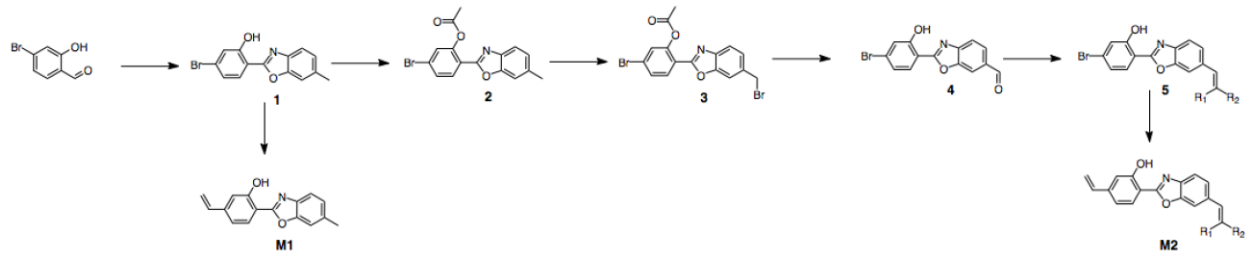

media.

Scheme 1. Synthesis of Li ion fluorescent sensors with tunable absorbance spectra. R groups in M2 represent strong electorn withdrawing groups.

Conclusions

Significant synthetic progress was made toward developing Li ion sensors with tunable emission spectra. Their synthesis and incorporation into binders will be finished next quarter, along with the study of their sensitivity for detection of Li ions in various environments. We will then begin incorporating these binders into actual electrodes and begin imaging their fluorescence with ultra-high resolution techniques through collaboration with LBNL as a first step towards their application to study SEI development. ORNL has proposed various time-resolved PL studies to probe how these materials bind to silicon.

References

1. J. Seo, S. Kim, S. Young Park, "Strong Solvatochromic Fluorescence from the Intramolecular Charge-Transfer State Created by Excited-State Intramolecular Proton Transfer", *JACS*, **2004**, *126*, 11154.

SEI Characterization: Lithium Silicate – Electrolyte Reactivity

Jaclyn Coyle (UC Boulder), Kevin Zavadil (SNL), Chris Apblett (SNL)

Background

This quarter, we have focused on collecting results from "soaking" experiments, where the silicon test samples (50nm thick Si over 500nm thick Cu on degenerate Si single crystal wafer, with Au/Ti backside contact) have been exposed to the Gen 2 electrolyte (without FEC) and the resulting surfaces analyzed using various techniques, including XPS, IR, and SEM. This supports the Q2 Milestone of "Have characterized (XPS, SIMS, IR, and Raman) the surface chemistry and composition of the SEISta model research samples after contact with the electrolyte, before cycling, including the nature of the electrolyte decomposition products".

Results

LixSiyO studies

Standard samples of thin film Si (50nm Si/500nm Cu/650um C-Si degenerate/100nm Ti/500nm Au) were prepared and diced using the methods previously described. These samples were then used to sputter deposit 50nm thick lithium silicates of varying compositions (SiO_2, $Li_2Si_2O_5$, Li_2SiO_3, and Li_4SiO_4) expected from the tie line on the Li-Si-O ternary for lithiation of SiO_2. These correspond to a 0, 1:1, 2:1, and 4:1 composition of Li:Si. Samples were then exposed to the gen-2 electrolyte (EC:EMC 3:7 1.2M $LiPF_6$) without FEC for varying lengths of time between 30 minutes and 3 days. These had no electrochemical component, so this study only probes the chemical reactions of the surface. Sample prep was convoluted by fluorine and carbon contamination in the samples discovered during XPS; data regarding these soaking experiments is shown as collected.

The first set of data is SEM imaging of the surface after exposure to the electrolyte for various times with a coating of silicate on the surface. Samples of the 1:1 ratio were exposed for various times, and their surface morphologies are shown in Figure 1. As can be seen, numerous small defects, likely the result of sputtering, initiate the growth of the SEI out from these positions, and the film is completely continuous after as little at 3 hours. As time extends, the film grows thicker, and within as little as 24 hours, structures start to emerge that indicate a lower layer of film in the darker regions, covered by a porous upper film layer, which are the lighter regions. This morphology continues to evolve out to the end of the 3 days of exposure to electrolyte.

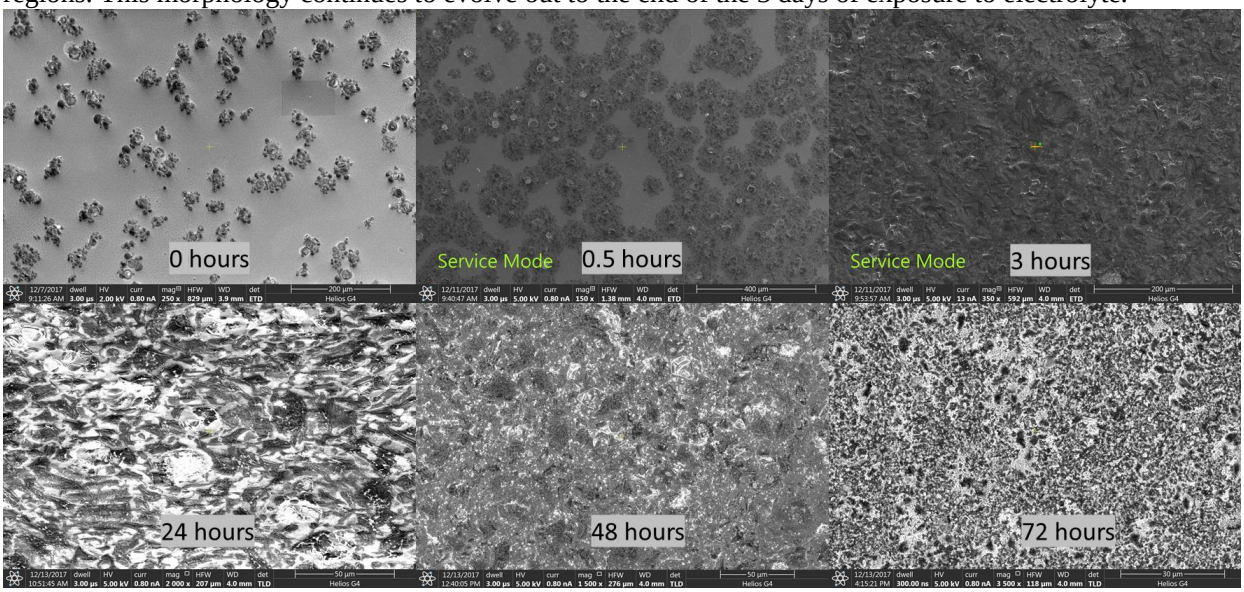

Figure 1: SEM images of Si surface with ~50nm sputtered $Li_2Si_2O_5$ model SEI exposed to gen 2 electrolyte for various times, showing the growth and structural evolution of the film just from exposure (no electrochemistry).

Soaking experiments of the 4:1 analyzed through ATRIR, however, show that while significant chemical evolution occurs in the SiO_2, almost no significant evolution of chemistry is observed even out to 72 hours in the 4:1 chemistry (see Figure 2). This may indicate that films with lower Li ratio (either SiO_2 or the 1:1) may have a different evolution of the SEI than films that are more higher in Li:Si ratio, and may be more chemically stable due to higher lithiation of the nonbridging oxygen bonds.

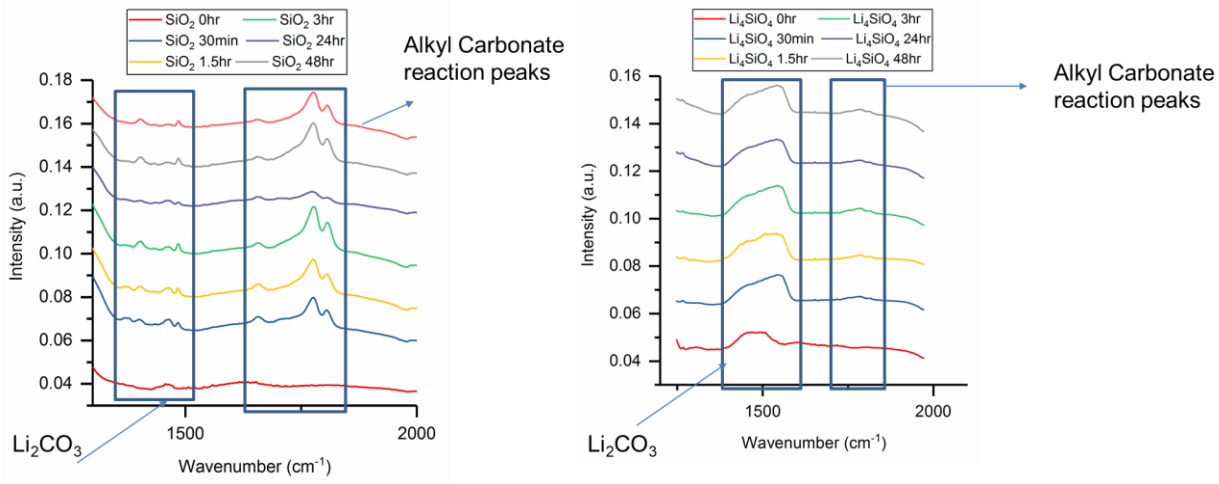

Figure 2: Comparison of ATRIR data on SiO_2 (left) and Li_4SiO_4 (right) after exposure to gen 2 electrolyte over time. Note that Li_4SiO_4 appears significantly less reactive for forming alkyl caronates, but may enhance the existence of lithium carbonate in the film.

Studies of intermediate Li:Si ratios using XPS after exposure to electrolyte for varying times suggests that there may be a marked time evolution on these compositions. Data for the carbon 1s and the phosphorus 2P peaks after varying amounts of soaking are shown in Figure 3. More work needs to be done, but these preliminary data show a decrease in both of these surface peaks between 30 minutes of exposure and 3 days of exposure. One possibility being explored is that a surface layer that is initially adherent forms, but that this

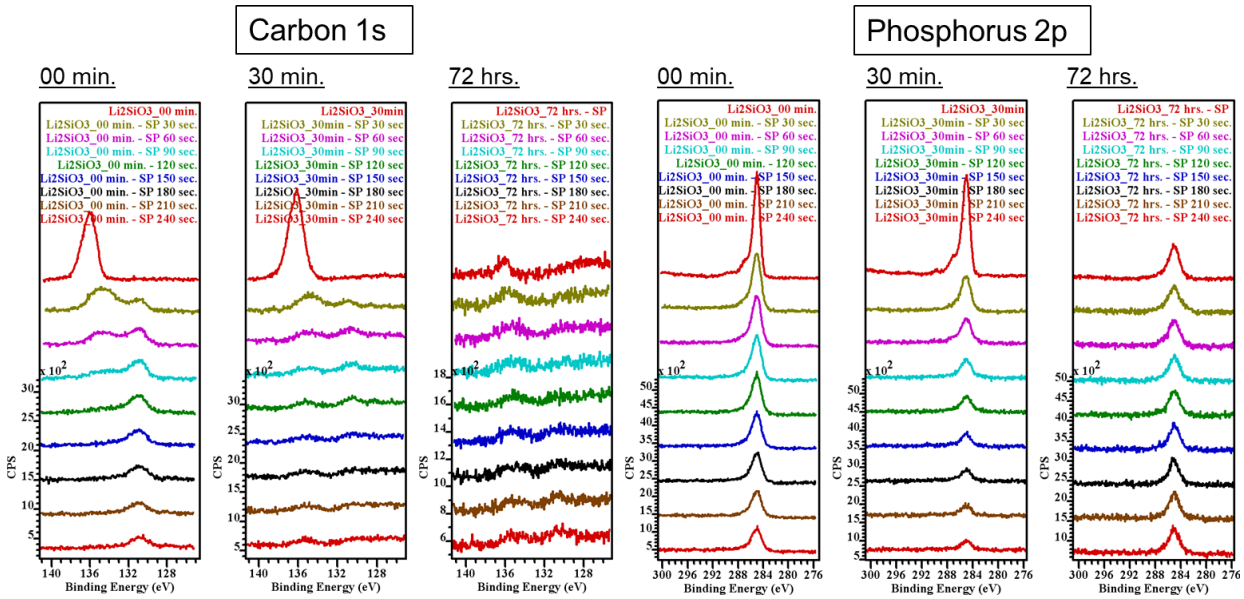

Figure 3: XPS analysis of 2:1 Li:Si film after exposure to electrolyte for various times. Note that the surface C and P peaks are markedly decreased with increased soaking time, suggesting removal of the film after soaking exposure and rinsing.

destabilizes as the film grows and becomes less adherent, and is ultimately washed away when the samples are rinsed for analysis.

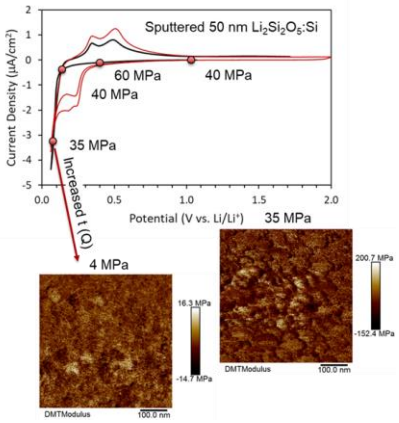

Figure 4: Electrochemical Atomic Force Microscopy (ECAFM) images of Li:Si 1:1 films on Si. Films initially have a modulus of approximately 35MPa when poised at ~60mV above Li, but degrade to 4MPa as lithiation proceeds.

Surface Exposure studies

This idea of a less adherent layer that is growing over time and ultimately destabilizes the SEI from the Si surface was further tested using electrochemical AFM techniques and poising at varying conditions while exposed to electrolyte. These series of experiments measured the modulus of the surface layer under various potential conditions, and then how the modulus evolved after a long exposure time under lithiating conditions for the substrate. The modulus of silicate films (in this case, the 1:1) did not appreciably change under various potential conditions initially, but if the cell was allowed to pass current under low overpotential to lithium, the modulus decreased significantly over time, suggesting a modification to the silicate film or the growth of an underlayer (Figure 4). While the impedance of the cells increased over time as the modulus decreased, it did not appear that the silicate itself changed in thickness. This can be seen in the SIMS data shown in Figure 5. The depth of the Si interface shifts to higher number of sputter cycles, indicating alloying of the Si with Li, but note the thickness and composition of the covering silicate is unmodified even after lithiation over time, suggesting the appearance of an interfacial layer that grows with continued lithiation.

Bolts and Cell Testing

The assembly of a rapid screening activity for determining rate limiting steps of the film growth has been assembled, comprised of a number of T cell test coupons configured for both variation of the silicate film composition and for temperature. Assembly of the first cells had very poor performance and cell disassembly showed discoloration of the PEEK isolation used in the cells. This behavior has been traced to a contamination in the electrolyte, likely stemming from storage in amber bottles. New sources of electrolyte have been obtained stored in polyethylene lined bottles, and the test rig is being assembled to replicate the soaking experiments with temperature and chemistry dependence, while mapping changes in impedance to an Arrhenius relationship to determine rate determining steps and begin to determine the initial states of film formation.

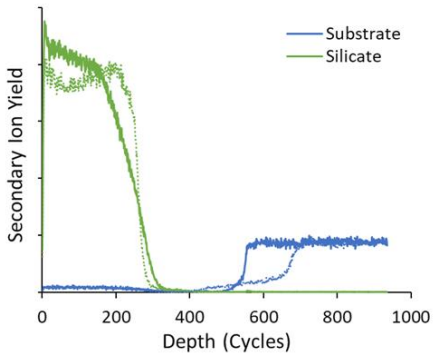

Figure 5: SIMS Yield vs. sputter cycle measurement of ion yields indicative of the Li:Si 1:1 film (green) and Si substrate (blue) both initially (solid lines) and after subjecting the film to a substantive lithiating total charge (dashed lines). The Si interface moves into the film, indicating alloying, but the overlaying lithium silicate does not appear to be changing thickness or composition.

Conclusions

Studies of the silicates exposed to the electrolyte are ongoing, but the initial hypotheses are that the composition of the silicate starting layer will direct subsequent evolution of the SEI formed by limiting or allowing sufficient Li+ penetration through the film to affect how the alloying process with the underlying Si occurs. In addition, the existence of a lower modulus interfacial layer between a stable, unmodified lithium silicate and the alloyed Si seems to be forming, and this more compliant layer may affect the mechanical integrity of the silicate layer over time.

SEI Characterization: Chemical reactivity of lithium silicide thin film with electrolyte (NREL)

Yun Xu (NREL), Jaclyn Coyle (CU Boulder), Andriy Zakutayev (NREL)

Background

Fluoroethylene carbonate (FEC) has shown the ability to improve cycle life of silicon anode materials, [1] However, the reason why FEC helps is still uncertain yet. Reduction potential of FEC is reported to be around 1.3V which is higher than the that of the other electrolyte solvents such as ethylene carbonate and diethylene carbonate. [2] FEC can be electrochemically reduced that it is reduced with current drive, or thermodynamically reduced on the surface of reducing agent with lower chemical potential such as the surface of lithium silicide. It is difficult to de-convolute the electrochemical and chemical reduction of FEC with electrode because of the buried lithium silicide after lithiation. Conventional way to study the lithium silicide with powders is difficult due the signal ratio coming from surface is low compared to that from the bulk, which makes the extraction of information from surface difficult. In this study, lithium silicide thin film is prepared by diffusion reaction from the evaporated lithium and sputtered silicon thin film. Chemical reaction between lithium silicide and electrolyte were directly measured by ATR_FTIR.

Results

Lithium thin films with different thickness (100nm, 200nm) was evaporated onto 50 nm silicon thin film on copper substrate. Specific capacity was calculated by the total mass of lithium and silicon. 100nm lithium //50nm silicon and 200nm lithium//50nm silicon thin film were calculated to be 33.1 ug and 26.5ug respectively. Both Gen 2 and 10wt% FEC added Gen2 (**FEC in short**) were studied in this work. Galvano-charge and discharge cycling were performed with coin cells with both electrolytes. Half cells were discharged to 50mV and charged to 1V at C/10 for 100 cycles. Electrolytes were dropped on the surface the lithium silicide thin film which was deposited on Pt coated silicon wafer. Attenuated Total Reflection-Fourier transform infrared spectroscopy (ATR-FTIR) was performed with a Bruker Alpha spectrometer, under argon atmosphere in a glovebox. Cycling performance of thin films with different lithium amount are shown in Figure 1. FEC improves the film stability **independent of the lithium amount**. 1st columbic efficiency (CE) was calculated by the 2nd charge capacity/1st discharge capacity. Both films retain 93% of the initial capacity after 100 cycles with FEC additive. But only 30% of capacity was retained with Gen2 electrolyte. CE with FEC is much stable compared to that with Gen2.

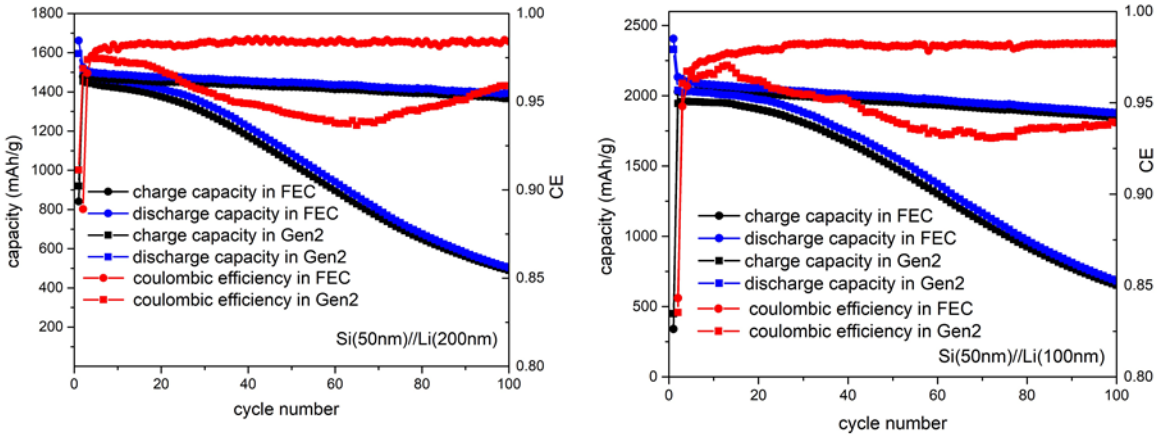

Figure 1. Cycling performance of thin films with both Gen2 and 10wt% FEC added Gen2.

To answer why FEC helps the cycle performance, we performed ATR_FTIR on the thin film of 200nm Li//50nm Si. Figure 2 shows the ATR_FTIR spectra of FEC and Gen2 treated lithium silicide. Peak assignment was refereed to previous ATR-FTIR study [3] of lithium metal immersed in electrolytes. FEC helps form the uniform surface and suppresses the decomposition of PF_6^-. Similar findings are observed in this study. More organic phases formed with FEC and more inorganic phases formed in Gen2. In addition, Gen2 generated more F^- contained phases than FEC. XPS also shows similar composition with ATR_FITR. This study shows that FEC, EC, DEC can be chemically reduced by lithium silicide which agrees with the previous computational work by Julibeth et al.[4] However, less LiF phase exists in FEC case, which is contradictory to the previous experimental and computational results.[4-5] This result suggest that chemical reduction may lead to different products compared to the electrochemically reduction.

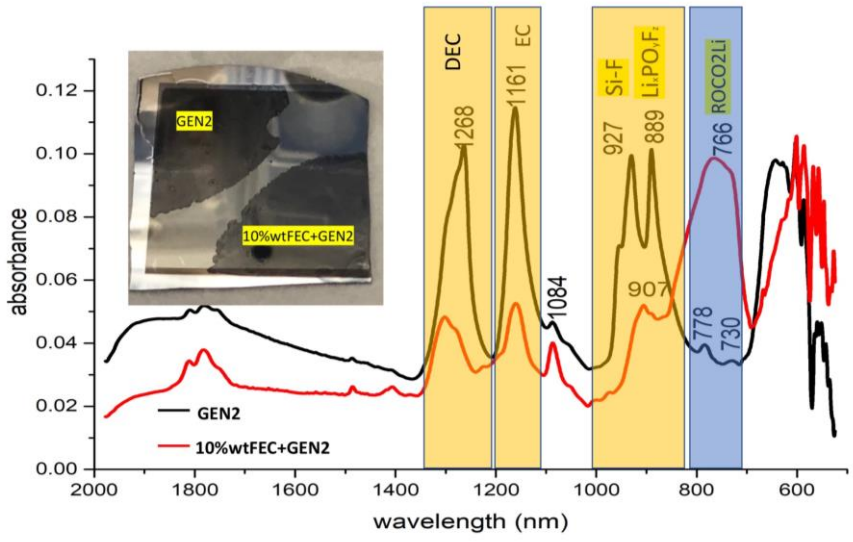

Figure 2. Inset pic: electrolyte drop on lithium silicide thin film on silicon wafer. ATR-FTIR spectra of the FEC and Gen2 treated lithium silicide surface.

Conclusions

Chemical reactivity of lithium silicide with electrolytes was studied by EX-situ ATR-FTIR. FEC additives and FEC-free electrolyte showed different reduction products. FEC resulted in more organic phases, while Gen2 resulted in more inorganic phase. From the galvanostatic cycling performance and columbic efficiency, we can make a conclusion that organic phases generated by FEC helps stabilize SEI layer.

References

1. Jaumann, T.; Balach, J.; Langklotz, U.; Sauchuk, V.; Fritsch, M.; Michaelis, A.; Teltevskij, V.; Mikhailova, D.; Oswald, S.; Klose, M.; Stephani, G.; Hauser, R.; Eckert, J.; Giebeler, L., *Energy Storage Materials* **2017,** *6*, 26-35.
2. Zhang, X.; Kostecki, R.; Richardson, T. J.; Pugh, J. K.; Ross, P. N., **2001,** *148* (12), A1341-A1345.
3. Kuwata, H.; Sonoki, H.; Matsui, M.; Matsuda, Y.; Imanishi, N., **2016,** *84* (11), 854-860.
4. Martinez de la Hoz, J. M.; Balbuena, P. B., *Physical Chemistry Chemical Physics* **2014,** *16* (32), 17091-17098.
5. Uchida, S.; Yamagata, M.; Ishikawa, M., *Journal of The Electrochemical Society* **2015,** *162* (3), A406-A412.

SEI Characterization: SEISta (Analytical Microscopy and Imaging Group, NREL)

Caleb Stetson, Seoung-Bum Son, Andrew Norman, Chun-sheng Jiang, Mowafak Al-Jassim (NREL)

Introduction

While the solid electrolyte interphase (SEI) is generally understood to form from applied electrochemical potentials during battery cycling, initial reactivity of the electrolyte in contact with the electrode surface has also been observed. In this quarter, investigation focuses on analyzing pre-cycling reactivity of electrolyte and electrode surface for model Si anode systems. To study this phenomenon, Si wafers with native and thermally grown SiOx were soaked in Gen2 electrolyte (1.2 M $LiPF_6$ in ethylene carbonate: ethylmethyl carbonate (3:7 by weight)). AFM was used to investigate the surfaces of these model systems and compare to the pristine surfaces before exposure to electrolyte. STEM was used to study if lithiation occurred and the nature of the reaction/SEI layer formed after one cycle in Gen2 electrolyte of a model Si wafer electrode covered with a 15 nm thick SiO_2 layer.

Moreover, surface precursor treatments (designed to stabilize initial SEI formation in battery cells) to Si wafers were characterized to investigate homogeneity and thickness of the layer formed by the chemical pre-treatment using AFM and scanning spreading resistance microscopy (SSRM).

Results

Native (~2 nm) and thermally grown oxide (50 nm) Si wafers were analyzed with AFM in a pristine

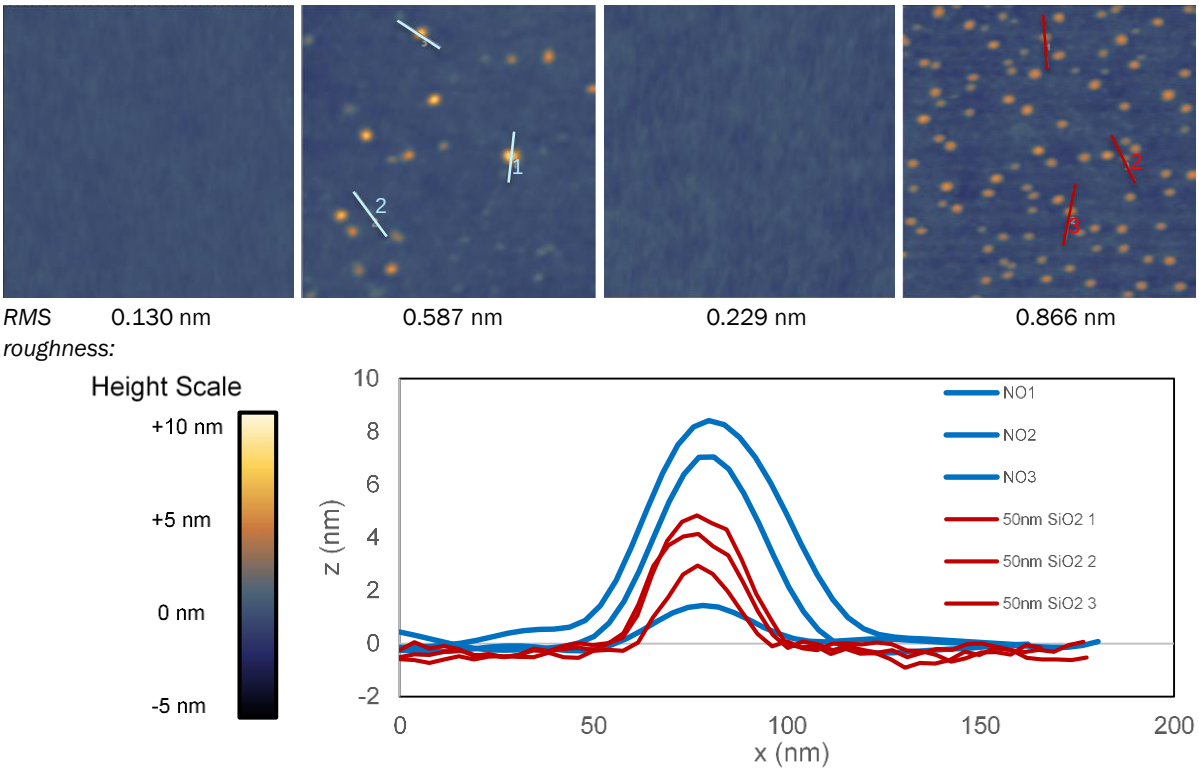

Figure 1. 1x1 µm AFM images from left to right: native oxide pristine surface, after soaking in Gen2 electrolyte, thermally grown 50 nm SiOx wafer pristine surface, after soaking in Gen2 electrolyte. A plot is shown displaying comparisons between linescans over surface islands on each sample.

After soaking in Gen2 electrolyte, island-like particles of possible electrolyte decomposition products and residual salts were found on both surfaces. However, on the 50-nm SiO_x surface, the particles showed greater density and more uniform size than on the native oxide surface, which is likely a result of rougher pristine surface with more initial adhesion and nucleation sites.

Precursor treatments of Si wafers were characterized with SSRM resistivity vs. depth profiling to determine thickness and homogeneity of the layers formed by the chemical reactions with precursors containing componenents as indicated in the x-axis in the graph (Fig. 2). The reactions formed layers with similar thicknesses of ~10 nm. Surface resistivity was analyzed with SSRM. AFM was also utilized to

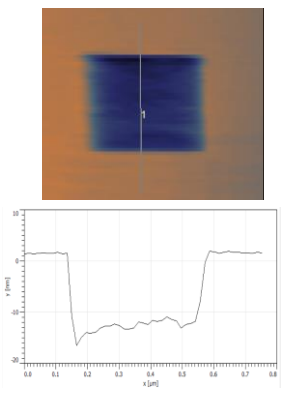

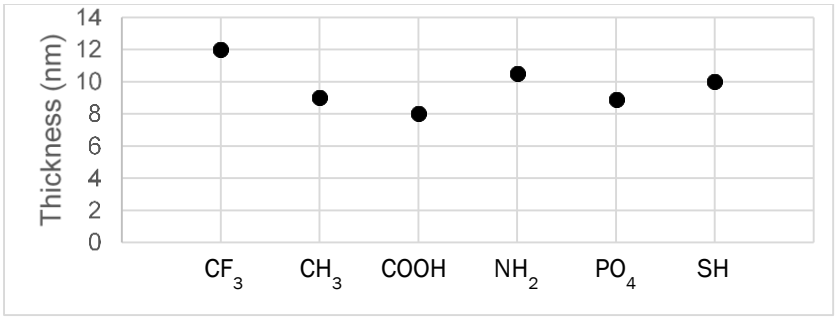

investigate the uniformity of surface pre-treatments.

Figure 2. Left: height image showing the top layer being milled away after depth profiling down to the Si interface. Si is recognizable by both its mechanical hardness and electronic conductivity compared to the layer formed by the treatment. Plot at right shows thicknesses of layersobtained from SSRM depth profiling.

A model Si anode system consisting of a 15 nm SiO_2 layer on wafer Si was selected for electrochemical cycling to determine if this thinner oxide allowed for diffusion of lithium. This sample was cycled in a coin cell with Gen2 electrolyte for one cycle, with 5 hours per half cycle at a constant current density of 22 μA cm^{-2}. The electrochemical data showed that lithiation had occurred. The cell was disassembled, the sample was removed and rinsed in DMC three times for 60 seconds, then transferred via air-free transfer to the focused ion beam (FIB) for sample preparation. A TEM cross-section was prepared and the sample was studied using scanning transmission electron microscopy (STEM) energy dispersive x-ray spectroscopy (EDS) and electron energy loss spectroscopy (EELS). STEM EDS mapping revealed the presence of carbon, fluorine, oxygen, and silicon in the ~ 25 nm thick solid electrolyte interphase (SEI). STEM EELS mapping, Fig. 3, revealed further details of the microstructure. A layered structure was revealed with a thin oxide layer adjacent to the Si wafer, followed by a thin carbon–rich layer, and finally a surface layer containing oxygen and fluorine.

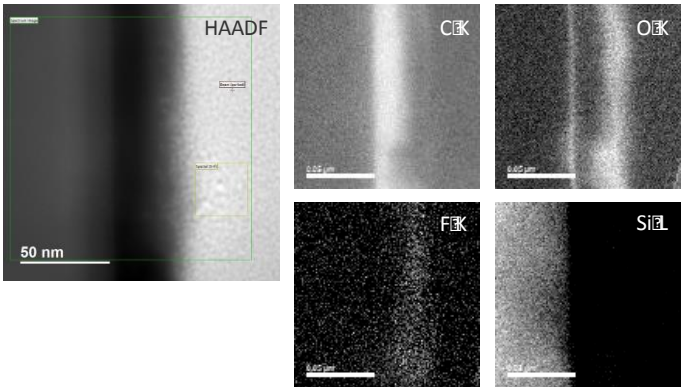

Figure 3. STEM EELS maps of SEI/reaction layer formed on Si wafer electrode with 15 nm SiO2 layer after one cycle in Gen2 electrolyte

Conclusions

Differences in reactivity of native oxide and thermally-grown SiO_x with Gen2 electrolyte were investigated with AFM, with results for each sample showing distinct island-like accumulations of possible electrolyte decomposition products and residual salts. Six chemical pre-treatments with different precursor of Si wafers were characterized with SSRM depth profiling to measure film thickness, electronic resistivity, and uniformity. STEM was used to determine the chemistry and microstructure of a model Si wafer electrode, covered initially with a 15 nm SiO_2 layer, after one cycle in Gen2 electrolyte.

SEI Characterization: Silicon Electrolyte Interface Stabilization (SEISta) [LBNL]

Ivana Hasa, Atetegeb M. Haregewoin, Liang Zhang, Jinghua Guo, Philip N. Ross and Robert Kostecki

Background

The primary objective of our effort is to clarify and understand the processes occurring at the silicon/electrolyte interface. The reductive decomposition of the electrolyte in lithium-ion systems employing silicon anodes is inevitable, since the working potential of the electrode is far below the electrochemical stability window of the electrolyte components. In principle, the insoluble decomposition products precipitating on the electrode surface, result into the formation of a passivating surface film which suppress further electrolyte decomposition.[1,2] However, the inherent instability of the silicon/electrolyte interface strongly inhibits the surface passivation, which is further endangered by the mechanical instability of the electrodes, which upon alloying with lithium experience a huge volume expansion responsible of active material cracking and consequent instability of the passivating film.[3]

A better understanding of the kinetic processes occurring upon cycling will enable an efficient implementation of silicon-based electrodes in high performance lithium-ion batteries. To accomplish this, we address the inherent non-passivating behavior of silicon model electrodes in organic electrolytes.

In order to de-couple the processes caused by the volume expansion and the inherent non-passivating behavior of silicon, the model electrodes of choice are represented by sputtered silicon thin film deposited on copper current collector, which represent the SEISta model research samples. The model electrodes, fabricated at ORNL, are constituted by 50 nm silicon thin film with a 3 nm native oxide surface layer.

Our effort in the last quarter has been mainly focused on the investigation of the interfacial properties of the silicon thin film electrodes and the characterization of the surface chemistry and composition upon cycling, including the nature of the electrolyte decomposition products.

Results

The electrochemical processes occurring at the silicon thin film/electrolyte interface have been investigated through ex-situ ATR-FTIR analysis. As reported in Fig. 1(a), the electrodes have been galvanostatically cycled at 5 µA cm^{-2} within the 0.05 V- 1.5 V vs Li^+/Li potential range. The electrochemical tests were performed in three electrode T-type Swagelok cells at room temperature employing glass fiber as separator and 1.2M $LiPF_6$ in EC:EMC 3:7 wt.% as electrolyte solution (Gen 2 electrolyte). The blue dots indicate the different state of charge at which the electrodes were recovered and subjected to the surface analysis as shown in the schematic in Fig. 1 (b). To avoid any alteration of the electrode's surface, the ATR-FTIR investigation has been performed under inert atmosphere and without any washing procedure to eliminate electrolyte residuals. Fig. 1 (c) reports the FTIR spectra of the silicon electrodes at 1.5V, 0.5V, 0.3V, 0.05V (lithiated state) and de-lithiated state at 1.5V. The comparison with the reference spectra reported for the wet and dried electrolyte (obtained as a result of the evaporation of EMC, which is the most volatile solvent), clearly indicates that mostly all the contributes can be related to electrolyte residuals. However, in the spectra of the fully lithiated electrode (0.05V), three new contributes are observed at about 1328 cm^{-1}, 1650 cm^{-1} and 1050 cm^{-1}, which upon further de-lithiation disappear. In an effort to avoid the electrolyte contribute and have a deeper insight

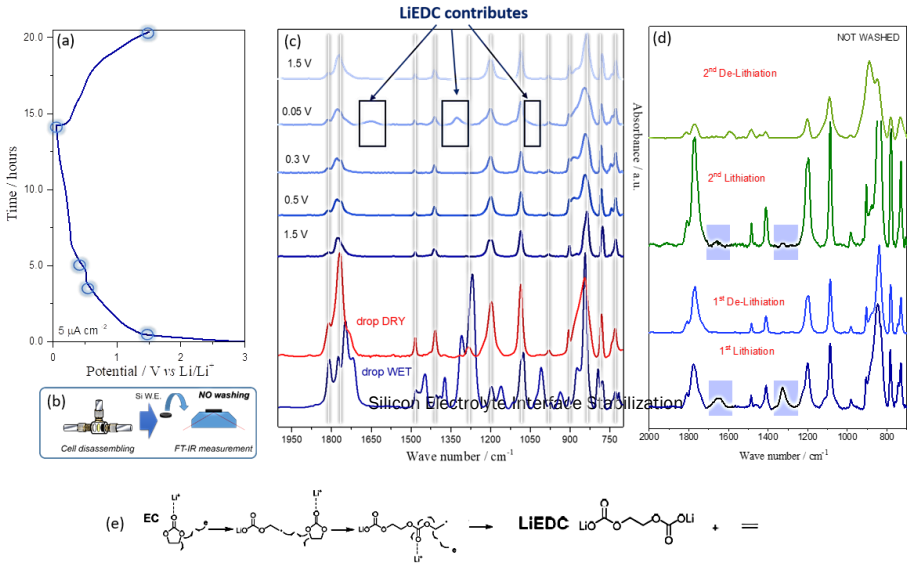

on the main electrolyte decomposition products, we adopted two main approaches. The first one consisting in a physical removal of the electrolyte residuals through a washing process, and the second one consisting in a subtraction of the electrolyte contribute by using the FTIR software. Both approaches led to the fundamental observation that the three main contributes observed appear only in the lithiated state and disappear upon de-lithiation. In addition, the peaks belong to non-soluble decomposition products of the electrolyte, being still present even after the washing process. The interesting behavior observed during the first galvanostatic cycles has been further investigated during the second cycle. Surprisingly, the three main peaks constantly appear and disappear upon (de-)lithiation also in the second cycle (see Fig. 1 (d)). According to previously reported literature [4], the new features are most likely related to the presence of lithium ethylene dicarbonate (LiEDC), which is the main decomposition product of EC based electrolyte following the decomposition reaction described in Fig. 1 (e). The presence of LiEDC has been further confirmed by using single wavelength Infrared near-field scanning optical microscopy, which allows the detection of single components at high resolution.

Figure 1. (a) First galvanostatic cycle of a silicon thin film electrode cycled in 1.2M $LiPF_6$ in EC:EMC 3:7 wt.% electrolyte at 5 µA cm^{-2} within the 0.05 V-1.5 V vs Li^+/Li potential range. (b) Schematic of electrode recovery for ex-situ ATR-FTIR analysis. (c) Comparison of ex-situ ATR-FTIR spectra of silicon thin films at different state of charge during the first cycle and electrolyte reference spectra. (d) Ex-situ ATR-FTIR analsysis of lithiated and de-lithiated electrodes during first and second cycle. (e) Decomposition pathway of EC and formation of LiEDC.[4]

Using a 1330 cm^{-1} excitation wavelength (which corresponds to an adsorption peak of LiEDC), a strong absorbance has been detected, while changing wavelength to 1360 cm^{-1} revealed no significant absorbance (data not reported here). The presence of LiEDC is not a new finding in lithium cells. Early studies conducted on the surface of Ni electrodes [4] and more recently on Si wafers [5], revealed the presence of LiEDC at potential approaching 0 V vs Li/Li^+, and also on metallic lithium [6].

However, our new results lead to a fundamental observation for a deeper understanding of the passivating properties of silicon electrodes. Indeed, the appearance and disappearance of LiEDC may be related to the inherent non-passivating behavior of silicon and to the instability of the surface layer formed upon cycling which is formed and decomposed in a dynamic mode. The "breathing" mode of the passivating layer on top of the silicon thin films has been also detected by X-ray absorption spectroscopy. The analysis of the Silicon L-edge (data not reported here) reveals the formation and thickening of a surface layer upon lithiation, which upon de-lithiation reduces considerably its thickness, thus further confirming the dynamic growth and disappearance of the surface layer.

Conclusions

The electrochemical properties of Si thin film model electrodes were studied accompanied by post-mortem analysis of the surface chemistry. The formation of LiEDC upon lithiation has been detected by ATR-FTIR, XAS and single wavelength Infrared near-field scanning optical microscopy. The results indicate a dynamic growth and disappearance of the passivating surface film. This fundamental observation represents a step forward the understanding of the inherent non-passivating behavior of silicon electrodes. The "breathing" effect of the surface film formed, most likely related to the formation and dissolution of LiEDC, suggests the latter one to be a fundamental component for the stability of the passivating layer.

References

[1] E. Peled, *J. Electrochem. Soc.*, **126**, 2047-2051 (1979).

[2] M. Winter, *Zeitschrift Für Phys. Chemie*., **223**, 1395-1406 (2009).

[3] M.N. Obrovac, V.L. Chevrier, *Chem. Rev.*, **114**, 11444-11502 (2014).

[4] G.V. Zhuang, K. Xu, H. Yang, T. R. Jow, P.N. Ross, *J. Phys. Chem. B*, **109**, 17567-17573 (2005).

[5] F. Shi, P.N. Ross, G.A. Somorjai, K. Komvopoulos, *J. Phys. Chem. C*,**121**, 14476-14483 (2017).

[6] D. Aurbach, Y. Gofer, M. Ben-Zion, P. Aped, *J. Electroanal. Chem.*, **339**, 451-471 (1992).

SEI Characterization: Electrochemical reactivity of the SEI (NREL)- FY18, Q2

Yanli Yin, Chunmei Ban (PI), NREL, Golden, CO

Background

The objective of this project is to develop a fundamental understanding of solid electrolyte interphases (SEI) for silicon (Si)-based electrode materials and provide practical strategies for stabilization of the SEI in Si-based electrodes. The SEI layer begins to form as soon as the Si electrode contacts the electrolyte. The SEI is comprised of the products from many reduction reactions of salts, solvents and impurities. These reduction reactions competes with each other; and the kinetics is heavily dependent on current density, overpotential and the catalytic properties of the electrode surface, finally determine the composition of a SEI. Regarding the silicon anode, the volume changes caused by the lithiation/delithiation process present new challenges. The continuous reduction of electrolyte may be attributed to the unceasing appearance of new surface during the volume changes, which can obfuscate the study of the interaction between the electrolyte and the Si surface. In order to decouple the interfacial chemistry from the interference of the volume changes, here, we aim to investigate the early-stage SEI chemistry before the Si lithiation process. This approach enables the study of the sole impact of early-stage SEI on the composition of SEI and the electrochemical behaviors. Furthermore, the information collected from the early-stage SEI could provide the new strategies to stabilize the Si electrode surface.

The intrinsically high sensitivity of SEI to the reaction environment and the surface structure and morphology has contributed to the measurement discrepancies, which causes significant difficulty in fully understanding the chemistry of SEI. Therefore, we have firstly established standard model Si electrodes, cleaning protocols, and cell fabrication procedures to elucidate the convoluted mechanisms of SEI on Si-based electrodes.

Milestones

- Define the formation of the early-stage SEI for the Si model electrode. (Jan 15th 2018)
- Demonstrate the effect of the electrolyte composition ($LiPF_6$ and LiTFSI based electrolytes) on the formation of the early-stage SEI . (Mar 30th 2018)
- Modify the surface of the Si model electrode with lithium carbonate (nonconductive) and carbon (conductive) coating and evaluate the coating impact on the formation of the early-state SEI. (Jun 30th 2018)
- Summarize the effects of the electrolyte composition and coating materials on the chemistry of the early-stage SEI. (Sept. 30th 2018)

Results

Experimental Method. Silicon model samples (denoted as SN) established in FY17 have been used in this study. In order to investigate the coating effect on the formation of SEI, we have coated the Si electrodes with the conductive carbon film (denoted as SNC) and the non-conductive lithium carbonate film (denoted as $SNCO_3$). All of the Silicon (Si) electrodes (½ inch x ½ inch) were cleaned with our established multi-step cleaning protocol to remove the surface grease, particles and organic residue. After cleaning, the electrodes were dried in vacuum oven at 100 °C prior to the cell fabrication. The electrolytes selected for this research are i) the saturated LiTFSI solution with EC:EMC solvents (3:7) (abbreviation "ST" used in the plots). ii) 1.2 mol/L LITFSI (abbreviation "TF" used in the plots) and iii) 1.2 mol/L $LiPF_6$ (abbreviation "G2" used in the plots) dissolved in the solution comprised of ethylene carbonate (EC): ethyl methyl carbonate (EMC) with the weight ratio of 3:7, respectively. All of the Si electrodes were used as work electrodes in the customized electrochemical cells, where the lithium metal was used as a counter electrode. 7 µl of the electrolyte was used in every cell; and the Celgard 2325 was used as a separator for the cell assembly.

Results and Discussion.

Galvanostatic lithiation and delithiation were performed on the Si electrodes, by using three cycling rates (5 µA, 11 µA and 22 µA). At each cycling rate, the cells were lithiated up to 2 hours and delithiated up to 1 V. Therefore, the cells, which were cycled at the same rate, have the same lithiation capacity. The potential-

capacity profile (V-Q) was plotted to analyze the electrochemical reduction reactions of the electrolyte during the lithiation and delithiation process. The voltage profile of cells by using the standard LiTFSF electrolyte has been displayed in Figure 1. Fig. 1a, b and c present the lithiation and delithiaion curves at the current of 5 μA, 11 μA and 22 μA, respectively. The plateau section of the lithiation curve is characteristic of lithiation of the crystalline Si, usually starts around or below 0.1 V. The electrochemical activities above the lithiation is ascribed to the reduction and decomposition of the electrolyte, which causes the irreversible capacity loss.

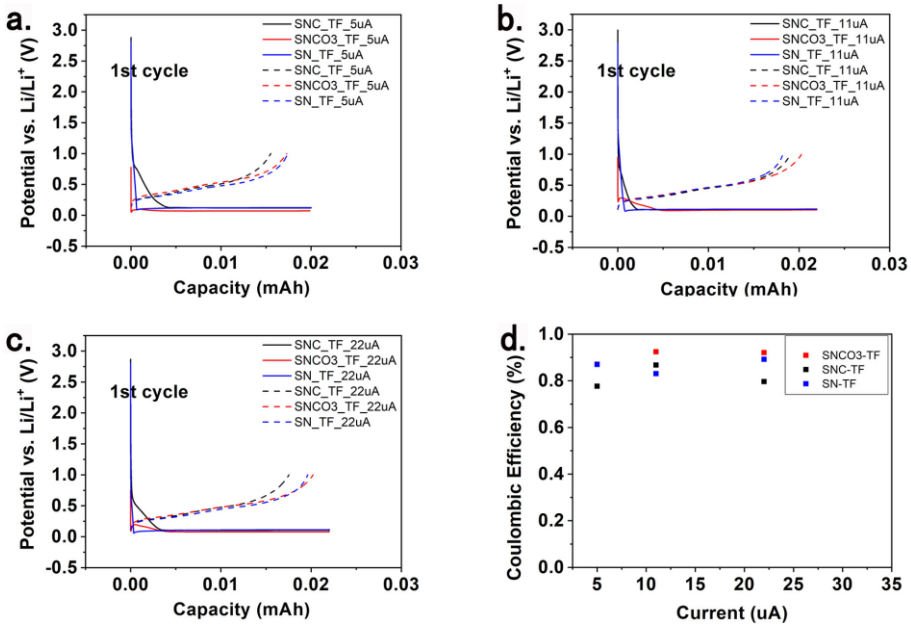

Figure 1. (a-c) The potential-capacity profile of Si electrodes with various coatings in the 1.2 mol/L LITFSI (EC:EMC=3:7); (d) The Coulombic efficiency of Si electrodes with various coatings at different currents.

Due to the instability of the electrolyte, the reduction and decomposition of the electrolyte start at pretty high voltage, around 1.3V vs Li/Li^+, for the pristine Si electrode. It is clearly shown that the coating materials have affected the surface reaction associated with electrolyte. By using the insulating coating (Li_2CO_3), the reduction reaction of the electrolyte has been greatly suppressed. However, the reduction has been accelerated when using conductive carbon coating. The products form the reduction reaction of electrolyte contribute to forming the early stage of SEI, considering the SEI continuously grows during lithiation. The information indicates that the reaction involved in the formation of the early-stage SEI can be kinetically suppressed with the insulating coating. The difference in the lithiation potential is also observed for the coated Si electrodes. The lithiation starts earlier in the carbon coated Si electrode, as compared to the pristine and carbonated coated electrodes. It indicates that the carbon coating does reduce the overpotential caused by the nonconductive surface species. Electrochemical impedance measurements are planned to obtain more information to correlate the surface impedance with the electrochemical behavior.

In addition, an reduction in electrochemical activity of electrolyte is also observed with increasing currents. It is expected that the structure and composition in the compact layer at the surface of Si electrodes is dependent on the electrochemical potential gradient. It is possible that less free solvent molecules are available for reduction at the surface, leads to the low reduction activities at a high current density. More spectroscopic study is planned to establish a better understanding of the solvation and solution structure at different current density.

The reduction behavior of the electrolyte becomes very different when increasing the salt concentration. As plots in Figure 2, all of the electrodes show very poor reversibility, suggesting the more side reactions related

to reduction decomposition of electrolyte. Here, we report the comparison in electrochemical properties when using different concentration and various current density. When a same coating material was applied on the Si electrode, the reduction reactivity of the electrolyte depends on the composition of the electrolyte, as summarized in Figure 3. More study is planned to investigate the effect of salt concentration on the reduction decomposition reactions.

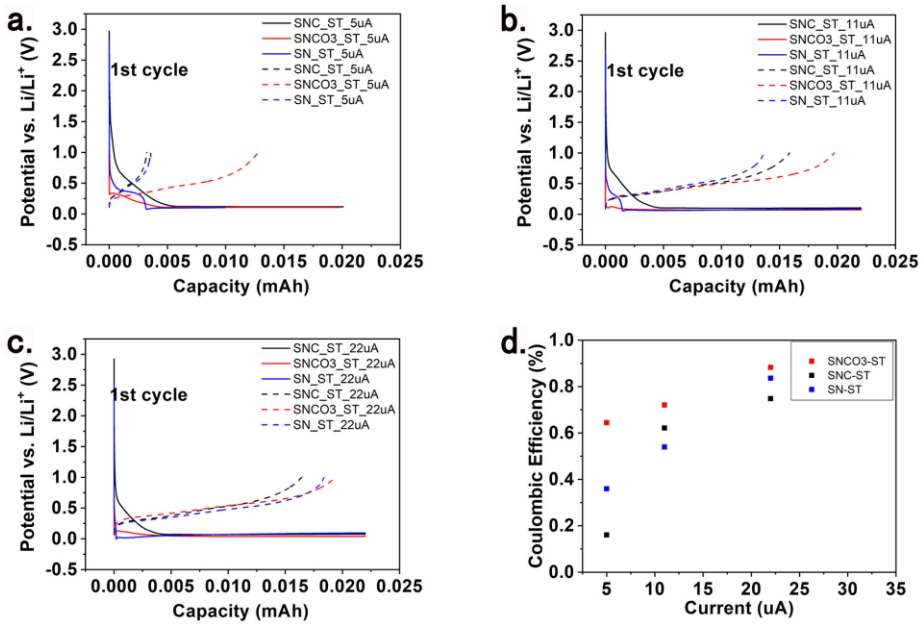

Figure 2. (a-c) The Potential-Capacity profile of the Si electrode with various coatings in the saturated LITFSI (EC:EMC=3:7) electrolyte ; (d) The coulombic efficiency of Si electrode with various coatings at different currents.

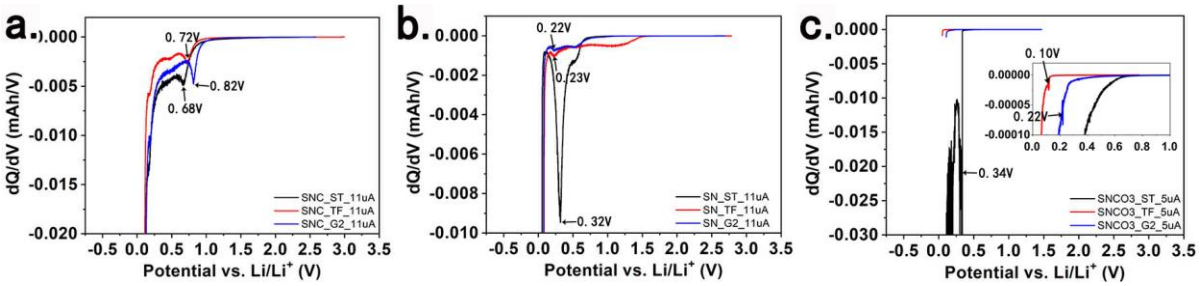

Figure 3. The differential capacity analysis of Si electrodes with different coatings (a) SNC, (b) SN (c) $SNCO_3$ in the various electrolytes.

Conclusions

The research in this quarter demonstrates the electrochemical behavior when using different electrolyte composition. In order to better understand the reduction reaction mechanisms of the electrolyte, we have tuned the surface conductivity by using insulating and conductive coating. The surface species on silicon show the

potential to modify the reaction of electrolyte and mitigate the irreversible capacity loss. It is expected that the coating layer may involve in the formation of SEI, thus provide an opportunity to manipulate the SEI chemistry for improving reversibility. It clearly show that the side reaction associated with electrolyte has been suppressed by using either high current density or the insulating coating. However, further investigation via other characterizing methods (FTIR, XPS and AFM etc.) are needed to establish a better understanding of the impact of electrolyte composition and surface species on the SEI chemistry.

SEI Characterization: Probing the Nanoscale Heterogeneity of SEI on Amorphous Silicon Using Tip Enhanced Raman Spectroscopy (TERS)

Guang Yang, Jagjit Nanda

Background

In last quarter, we reported the chemical signature of the SEI from the TERS measurements and analyzed the changes in the surface topography of SEI with the chemical compositional maps (TERS) to highlight the various SEI phases which are Raman active. The components of SEI on silicon surface is by nature complicated, and the Raman peak assignment is non-trivial. To verify the spectra of species from the TERS spectra of amorphous Si (a-Si) cycled at different numbers (1-cycle, 5-cycle and 20-cycle), we further reviewed and Raman band assignment for each sample. In addition, the results were compared with those obtained from the IR spectra. TERS mapping was implemented on a pristine amorphous silicon before cycling, providing the modes which could potentially convolute with some of the SEI Raman bands for cycled a-Si sample. The TERS spectra/mapping of the pristine a-Si indicates that sputtered Si on copper electron collector has heterogeneous distribution of lattice modes. A manuscript for the first spectral study of SEI in nanoscale on silicon surface using TERS is in preparation. Its sister work– using TERS to depict SEI on Si/SiO2 wafer samples of various cycle numbers is ongoing.

Results

Amorphous silicon (20 nm in thickness) was sputtered on the copper electron collector at ORNL and cycled as per the procedure finalized by the round robin team of SEIsta. TERS experiments were performed using a HORIBA Xplora Nano Raman Platform integrated with AIST-NT SPM system (laser wavelength = 532 nm and the objective was 100x/0.7 N.A.) The laser power was set at 100µW. The TERS tip was fabricated by thermal evaporating 2 nm chromium on commercial Bruker silicon tip (26 N/m, 300 kHz), followed by coating a 40 nm silver layer. A thin aluminum protection was coated on tip apex. IR spectrum of each sample was collected from a Fourier Transform Infrared (FTIR) spectrometer (Bruker, ALPHAII) with a diamond attenuated total reflection (ATR) accessory. The wavenumber of each spectrum was between 4000 and 400 cm^{-1} with 128 scans and 2 cm^{-1} resolution. The IR measurements were performed in an Ar-filled glove box (O_2 and H_2O < 0.1 ppm) to prevent the air exposure. All TERS measurements were performed in a special Ar-compatible antechamber to avoid air exposure.

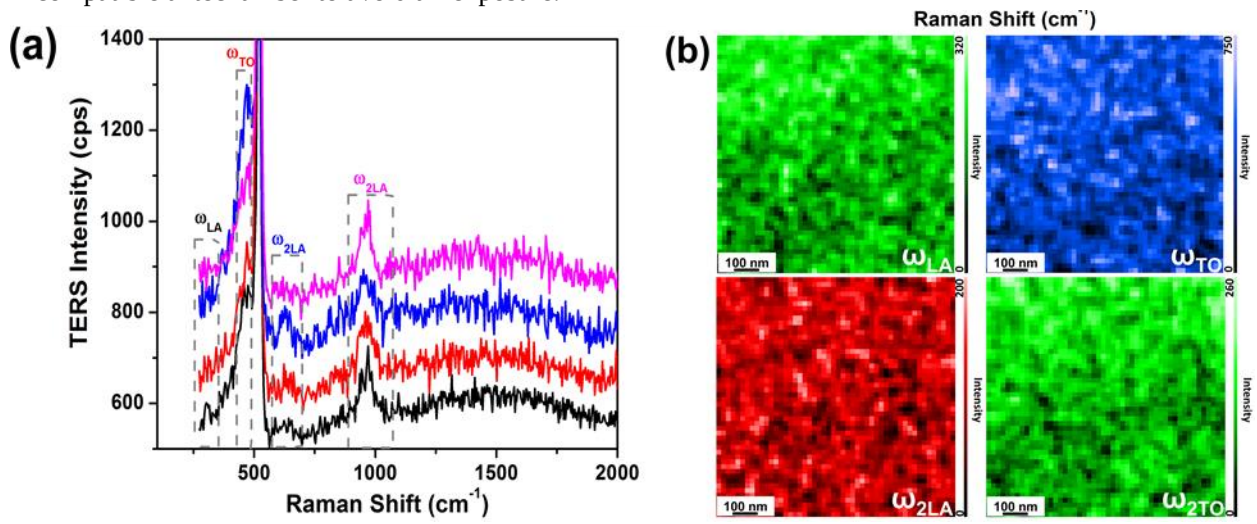

Figure 1 (a)TERS spectra taken from pristine a-Si on various locations corresponding to the maximum intensity for each mode. (b) TERS mapping of each lattice mode for a-Si.

The TERS spectra of pristine amorphous silicon (a-Si) exhibits four distinguished bands (Figure 1a) – in the low frequency end, the band at 306 cm^{-1} corresponds to the longitudinal acoustical mode (ω_{LA}), whereas the band shoulder at 472 cm^{-1} is ascribed to the transverse optical structure of a-Si (ω_{TO}). [1] A weak shoulder observed at 635 cm^{-1} for pure a-Si could be due to the overtone (ω_{2LA}) of the a-Si ω_{LA}, which was found at 610 cm^{-1} based on the normal Raman spectroscopy. [1] The band at 963 cm^{-1} is due to the overtone (ω_{2TO}) of the main a-Si ω_{TO}. The sharp peak of the most intensity at 520 cm^{-1} is assigned to crystal silicon (a-Si), which is from the TERS tip. Interestingly, the spatial distribution of those bands related to a-Si is heterogeneous in the sample plane (Figure 1b), which should be due to the heterogeneous rough surface of a-Si layer sputter coated on copper substrate (this information will be shown in the manuscript in preparation). Note that the ω_{2LA} for pure a-Si could overlaps with the secondary band of the crystal silicon (c-Si) tip. However, a careful inspection of the TERS spectra on the TERS tip indicats that the secondary c-Si band was not distinguishable, although the primary 520 nm c-Si was observable for this spectrum. Interestingly, this band did not show up for a-Si sample using standard Raman spectrum. This might be due to that the tip surface has a thick coating layer (~50 nm Cr+Ag+Al versus the 7 nm Si tip apex) and also due to the low laser power (100 μW). The TERS spectra of the pristine a-Si sample indicated to us that more careful analysis on the band assignment was necessary for the cycled a-Si samples. It is noteworthy that as such low laser power normal micro-Raman cannot detect any signal from the SEI.

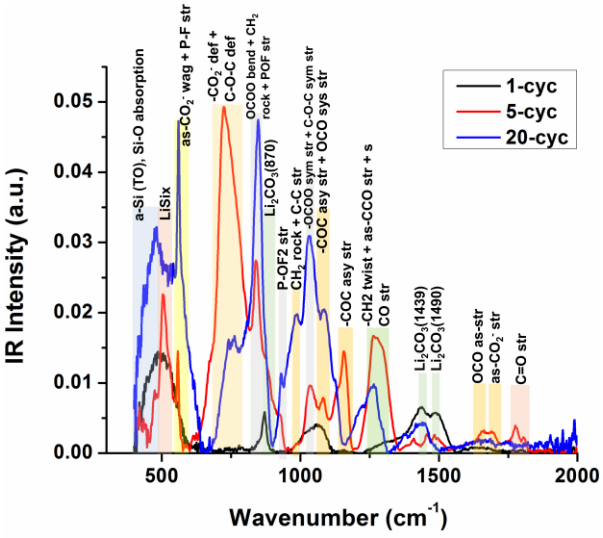

Figure 2 IR spectra taken from different a-Si samples and the band assignment

As comparison between the IR and TERS spectra for the a-Si of x5 and x20 cycles is still ongoing, we are solely focused on x1 a-Si sample here. The IR spectra of all samples are shown in Figure 2. For the 1-cyc a-Si sample, the major SEI component is lithium carbonate (Li_2CO_3), as the IR spectrum of this sample has a sharp band at 870 cm-1, which is contributed from the hybrid mode of longitudinal optical (LO) and transvers optical (LO) acoustic modes. 2 Notably, this band was assigned to the residual PF6- stretching mode by Ref 3. However, we do not see other featured bands assigned to the residual electrolyte molecules (e.g. C=O stretching modes for EC at 1735 cm-1 and 1753 cm-1). 4 Two other modes ascribed to Li2CO3 (1439 cm-1 and 1490 cm-1) are also observed,3 elaborating that Li_2CO_3 was enriched on the 1-cyc sample surface.

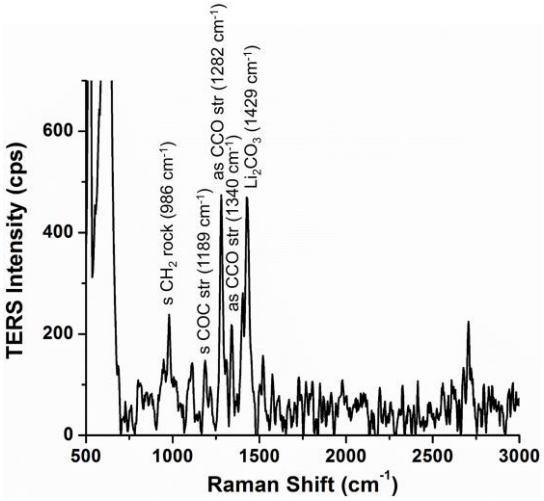

Figure 3 A TERS spectrum taken from 1-cyc a-Si

In contrast, the TERS spectra taken from the 1-cyc a-Si surface indicates the existence of other SEI spices. Figure 3 shows such a spectrum taken from organic species enriched region (TERS mapping not shown). It is obvious that besides the 1429 cm^{-1} Raman band(assigned to Li_2CO_3) bands corresponding to the oligomer poly (ethylene oxide) like species are also distinguishable. This demonstrates that the SEI vibrational information provided by TERS is highly localized, different than that of the bulk SEI measured by IR.

Conclusions

The benchmark TERS mapping was implemented on a pristine a-Si sample. IR spectra of a-Si of different cycle numbers indicate that the SEI is of different composition for each a-Si sample. The comparison between the IR spectrum and the TERS spectrum for the 1-cyc sample indicates that the SEI composition analyzed by IR could be intrinsically different than that measured from TERS.

References

1. Smith Jr, J.; Brodsky, M.; Crowder, B.; Nathan, M.; Pinczuk, A., Raman spectra of amorphous Si and related tetrahedrally bonded semiconductors. *Phys. Rev. Lett.* **1971,** *26* (11), 642.

2. Buijs, K.; Schutte, C., An infra-red study of the hydrates of sodium carbonate. *Spectrochim. Acta* **1961,** *17* (9-10), 917-920.

3. Zhuang, G. V.; Yang, H.; Blizanac, B.; Ross, P. N., A study of electrochemical reduction of ethylene and propylene carbonate electrolytes on graphite using ATR-FTIR spectroscopy. *Electrochem. Solid-State Lett.* **2005,** *8* (9), A441-A445.

4. Guang Yang, I. N. I., Rose E. Ruther, Robert L. Sacci, Veronika Subjakova, Daniel T. Hallinan, Jagjit Nanda, Solvation Structure of Lithium-Ion Battery Electrolytes using Gap Mode Surface Enhanced Raman Spectroscopy. *Submitted to ACS Nano* **2018**.

SEI Characterization: Understanding and Design of the Si SEI from Coupled Molecular Dynamics – First-principles Calculations (UC Berkeley)

Kristin Persson (UC Berkeley)

Background

Our examination of the Si anode reactions includes modeling of the solvation structures within the bulk electrolyte, bulk anode, and the interfacial reactions. We first investigate candidate reaction pathways by examining the solvation structure of the Li ion and electrolyte molecules in the bulk electrolyte and at the interface. As part of the effort, we will elucidate the solvation structure, reduction reactions and the SEI formation process of the electrolyte system. Current research focuses on the formation of the SEI and its constituents, but fewer publications exist on modifications to the bulk Si. Dopants and alloys can be an effective way of modifying electrochemical properties. Our efforts will focus on identifying systems with lower volumetric expansion, faster Li ion kinetics and improved SEI formation.

Results

The solvation behaviors for $LiPF_6$ in pure EC or EC with different concentrations of FEC were investigated based on previous quarter's research. The OPLS potential was selected for the molecular dynamics (MD) simulations. Two different concentrations (1.0 M and 1.2 M) and three ratios of FEC additive (0, 5, 10%) were considered (Figure 1.a). All the systems have approximately the same total coordination number of ~5.8, while it slowly decreases when adding a higher amount of FEC. According to experimental FTIR and NMR[1-2], a similar system (1.0 M $LiPF_6$ in PC) has a coordination number of ~4.7 and >5. Hence, with higher permittivity and smaller size, EC solvent molecules may exhibit higher coordination number, which matches our simulation results. Furthermore, a higher proportion of FEC resulted in higher amount of FEC and PF_6^- anion in the first solvation shell, resulted in a higher amount of F-contained species and a higher ratio of contact ion pair (CIP) ratio. Interestingly, we also found that the CIP ratio in bulk increases from 0.07 to 0.3 with temperature increasing from 300 K to 400 K. Consequently, the reduction potential and deposition kinetics of the electrolyte will be impacted. In addition, the ion transfer process is influenced.

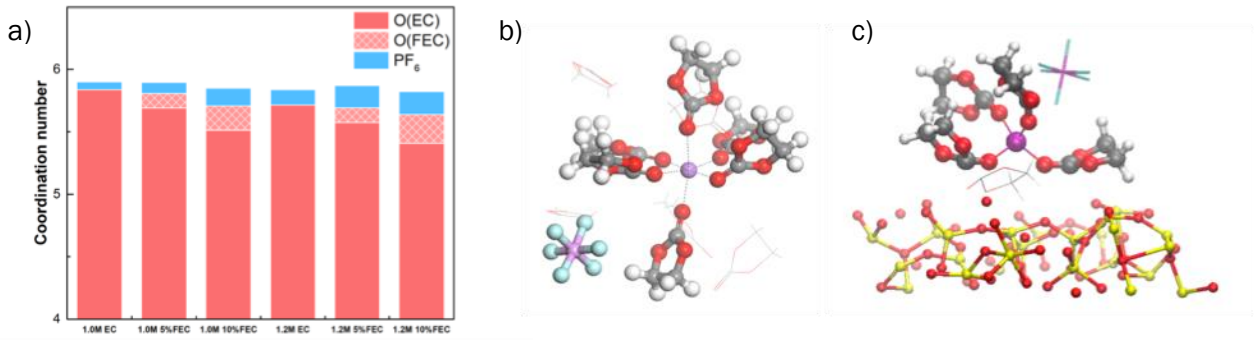

Figure 1: a) Calculated Li+ ion coordination number for 1.0/1.2 M LiPF6 in pure EC or EC with 5/10% FEC additive. Structures of EC molecules around a Li ion b) in bulk and c) at interface

Interfacial properties of ions/electrolyte molecules of $LiPF_6$/EC at the Si anode at the initial charging step are studied via with classical MD. We first investigated the solvation structure of the electrolyte molecules close to the interface. 1 M $LiPF_6$ in EC with OPLS force field is employed as the electrolyte, and neat crystalline Si with native silicon oxide layer as the anode. At 400K, We observed a reduction in the number of EC molecules participating in the Li ion solvation structure comparing bulk to interface, from CN ~ 6 to ~ 4 (Figure 1.b and c). At the interface the significant interaction between oxygen at the SiO_2 interface and Li ion reduces the CN of EC from 5.5 to 2.5, but the CN of Li-F becomes greater at interface from 0.4 in bulk to 1.2. This means that on average, lithium ions are more likely to exhibit contact ion-pair at the interface with CIP ratio of ~ 0.65 as

compared to the ~ 0.3 bulk ratio. Further, solvation structure at the charged electrodes will be calculated and compared to the neutral cases.

I.Table-1: Calculated reduction potential of the first solvation shell clusters obtained from MD simulations

Structures	Reduction potential
EC + e- → EC-	0.21 V
FEC + e- → FEC-	0.59 V
Li-(EC)4+ + e- → Li+-FEC-	0.51 V
Li-(EC)3(FEC) + + e- → Li+-FEC-	0.55 V

To probe the influence of the transition of solvation structures, the reduction potentials for the first solvation shell clusters were further calculated with 6-31+g* level quantum chemical calculation, as shown in Table 1. For free EC and FEC molecules, FEC exhibits higher reduction potential (0.59 V) as compared with EC, indicating that FEC is thermodynamically favorable to reduce at the anode surface and form SEI. Numerous amount of experimental studies[3-4] have proved that the SEI formed with FEC is more stable and have better electrochemical performance. With FEC included in the solvation shell, the reduction potential would increase from 0.51 V ($Li\text{-}(EC)_4^+$) to 0.55 V ($Li\text{-}(EC)_3(FEC)^+$), also in favor of FEC reduction.

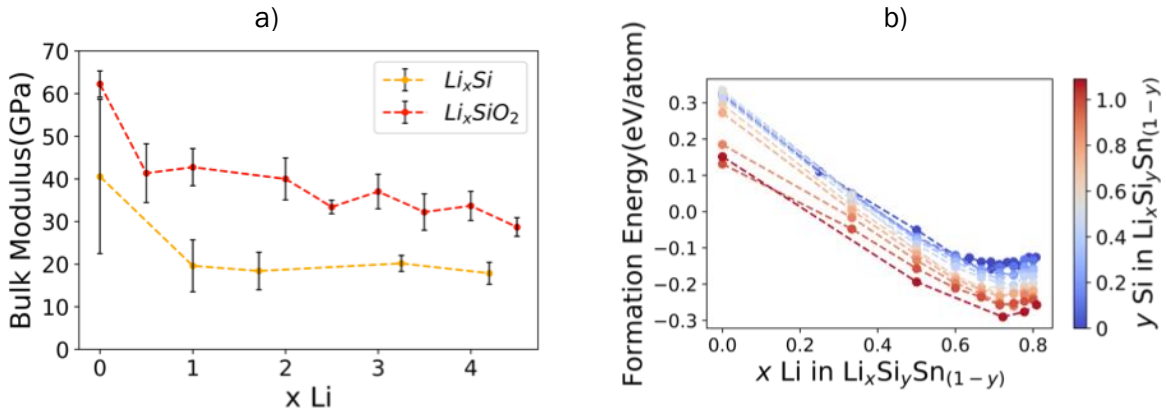

Figure 2: a) Bulk modulus of lithium silicates and lithium silicides. b) Formation energies of lithiated Si-Sn alloys.

Computation of the bulk moduli shows that lithium silicates are stiffer than the silicides. The higher modulus of the silicates suggests that the native SiO_2 oxide is less accommodating to expansion. As Li penetrates into the Si and forms Li_xSi, the volumetric expansion will build internal pressure, ultimately resulting in fracture of silicate layer. This is consistent with two observations. First, that the particles that make up a Si electrode crack during the first few lithiation cycles and expose more surfaces, this is especially seen in Si films. Second, the SiO_2 layer can be used restrict expansion of the silicide phases, as demonstrated by Wu et al. when surrounding the exterior surface of a Si nanotube with a SiO_2 to prevent outward expansion of the Si interior during lithiation [5]. In the prior quarter, we demonstrated improvement in Li-mobility when Si is alloyed with Ge or Sn. Here, we expand further and investigate a range of Si:Sn ratios from 10% to 90%. The formation energies of the Si-Sn alloys through lithiation follow similar trajectories, although higher Sn content are found to be favored. Consequently, the voltage of the higher Sn content electrodes will also be higher, in agreement with previous experimental work[6]. Further studies on the diffusivities of these alloys are underway.

Conclusions

1. The trend of EC solvation number of Li in EC is found to be 6 in bulk, and it reduces to 4 at the interface. Interaction between SiO_2 and electrolyte results in higher CIP ratio at the interface. Higher proportion of FEC in solvents resulted in higher amount of FEC and PF_6^- anion in the first solvation shell, resulting in a higher CIP ratio.

2. With FEC included in the solvation shell, the reduction potential would increase from 0.51 V (Li-$(EC)_4^+$) to 0.55 V (Li-$(EC)_3(FEC)^+$), also in favor of FEC reduction.
3. We demonstrated a favored formation of higher Sn concentration in Si-Sn alloys, resulting in a higher voltage.

References

[1] Chapman, N.; Borodin, O.; Yoon, T.; Nguyen, C. C.; Lucht, B. L., Spectroscopic and Density Functional Theory Characterization of Common Lithium Salt Solvates in Carbonate Electrolytes for Lithium Batteries. The Journal of Physical Chemistry C 2017, 121 (4), 2135-2148.

[2] Seo, D. M.; Reininger, S.; Kutcher, M.; Redmond, K.; Euler, W. B.; Lucht, B. L., Role of Mixed Solvation and Ion Pairing in the Solution Structure of Lithium Ion Battery Electrolytes. The Journal of Physical Chemistry C 2015, 119 (25), 14038-14046.

[3] Sina, M.; Alvarado, J.; Shobukawa, H.; Alexander, C.; Manichev, V.; Feldman, L.; Gustafsson, T.; Stevenson, K. J.; Meng, Y. S., Direct Visualization of the Solid Electrolyte Interphase and Its Effects on Silicon Electrochemical Performance. *Advanced Materials Interfaces* **2016,** *3* (20), 1600438.

[4] Schroder, K.; Alvarado, J.; Yersak, T. A.; Li, J.; Dudney, N.; Webb, L. J.; Meng, Y. S.; Stevenson, K. J., The Effect of Fluoroethylene Carbonate as an Additive on the Solid Electrolyte Interphase on Silicon Lithium-Ion Electrodes. *Chemistry of Materials* **2015,** *27* (16), 5531-5542.

[5] Wu, H.; Chan, G.; Choi, J. W.; Ryu, I.; Yao, Y.; McDowell, M. T.; Lee, S. W.; Jackson, A.; Yang, Y.; Hu, L.; Cui, Y. Stable Cycling of Double-Walled Silicon Nanotube Battery Anodes through Solid–electrolyte Interphase Control. Nat. Nanotechnol. 2012, 7 (5), 310–315.

[6] Hatchard, T. D.; Dahn, J. R. Study of the Electrochemical Performance of Sputtered Si[sub 1−x]Sn[sub X] Films. J. Electrochem. Soc. 2004, 151 (10), A1628.